The Pennsylvania State University

The Graduate School

Intercollege Graduate Degree Program in Ecology

PHAKOPSORA PACHYRHIZI UREDINIOSPORE ESCAPE FROM A SOYBEAN CANOPY

A Thesis in

Ecology

by

Jeremy Martin Zidek

Submitted in Partial Fulfillment
of the Requirements
for the Degree of

Master of Science

August 2007

Jeremy Martin Zidek

The thesis of Jeremy Zidek was reviewed and approved* by the following:

Scott A. Isard
Professor of Aerobiology
Thesis Advisor

Erick D. De Wolf
Professor of Plant Pathology

David A. Mortensen
Professor of Weed Ecology

Joseph Russo
President of ZedX, Inc.

Barbara J. Christ
Professor of Plant Pathology
Head of the Department of Department of Plant Pathology

*Signatures are on file in the Graduate School

ABSTRACT

Predicting the potential arrival of soybean rust through the use of aerobiological modeling may help growers decide if a fungicide application is needed. Many of the variables that govern aerobiological transport of *Phakopsora pachyrhizi* from one location to another are well understood. However, *P. pachyrhizi* spore escape from a soybean canopy has received little attention. The objectives of this research were to 1) estimate the proportion of released *P. pachyrhizi* spores that escape a soybean canopy and relate this value to atmospheric turbulence and canopy structure, 2) create concentration profiles of spores and particles and estimate vertical fluxes out of the canopy, and 3) provide a descriptive assessment of the directional and spatial components of movement for spores and particles in and above the canopy. The findings from this research will enhance our ability to predict spore movement of this important plant pathogen.

Spores were collected for 15-minute intervals near the center of a severely diseased field of soybeans at the University of Florida, North Florida Research and Education Center in Quincy, FL. Spores and spore surrogates (paint chip particles) were also sifted onto healthy canopies and were collected in the same manner. An experiment was also conducted at the Russel E. Larson Agricultural Research Farm at Rock Springs, PA using only particles. Rotorod samplers were placed on four vertical towers at heights relative to canopy height, h, at the following levels: 0.5 h, 1.0 h, 1.5 h, and 2.5 h. The towers were situated in a 3.0 x 3.0 m square. Atmospheric turbulence was measured using a 3-dimensional sonic anemometer (CSAT3). A total of 3 experiments consisting of 37 trials were conducted during the summer of 2006.

The measurements indicated that mechanical atmospheric turbulence, canopy structure, and atmospheric stability were important predictor variables for the proportion of released spores that escape a soybean canopy. The measurements also indicated, especially for collected spores that were released under ambient environmental conditions, that as atmospheric turbulence increased, the vertical escape flux of spores from a soybean canopy also increased. During the Pennsylvania experiment, the trials were conducted over the course of a season, and the number of particles moving inside the canopy was the most important variable governing the vertical escape flux of particles from a soybean canopy. This was attributed to the change in canopy structure over the course of the season. The measurements also indicated that the strength and direction of the maximum wind gust was an important factor in determining spore transport in and just above the canopy.

TABLE OF CONTENTS

LIST OF FIGURES

LIST OF TABLES

ACKNOWLEDGEMENTS

I would like to thank my advisor, Dr. Scott Isard, for giving me the opportunity to pursue a graduate degree in a field that is interesting and challenging to me. I would also like to thank the other members of my committee, Dr. Erick De Wolf and Dr. Dave Mortensen for their support and help with the research questions, and Dr. Joseph Russo for his help and support for my research as well as my career endeavors. I would like to thank Ash Bennett for his help in writing the leaf area index program.

I would like to thank the agencies and other universities responsible for funding my research project and providing field space and technical support. The USDA provided the necessary funding to complete the research project, I would like to thank Tim Grove, Justin Dillon, and everyone at the Russel E. Larson Agricultural Research Farm for helping construct my equipment, provide field space, and plant and spray the soybean field. I would like to thank Dr. Jim Marois, Dr. David Wright, and everyone at the University of Florida, North Florida Research and Education Center in Quincy, FL for providing research support, field space, and the ability to work with live soybean rust spores.

Finally, I would like to thank all of the people who have provided support throughout my time in graduate school. I would like to thank my parents for providing moral and financial support. My girlfriend, Smaro Kokkinidou, has always provided support and has made my time in graduate school very enjoyable. I would also like to thank the friends who have helped me through graduate school, Nick Dufault, Jim Brosnan, Kate Brosnan, Maria Velez, Katelyn Tilley, Vasilis Bitas, Jose Santa-Cruz, Rachel Melnick, and Annisa Demers.

Chapter 1

Introduction

1.1 History

Asian soybean rust (*Phakopsora pachyrhizi*) has spread rapidly and has the potential for causing severe yield losses making it the most destructive foliar disease of soybean (*Glycine max*) (Miles et al., 2003). Soybean rust has moved from the Eastern Hemisphere to South America and more recently into the United States. It has been a major disease of soybeans in the Eastern Hemisphere for decades, causing yield losses as high as 40% in Japan (Kitani and Inoue, 1960). In field trials in Taiwan, the numbers of pods per plant at growth stage R6 in unprotected treatmenats were reduced by as much as 40%, and the seed growth rate from R4 to R7 was reduced by 40-80% (Yang et al., 1991). Soybean rust has also affected soybean production in Australia and more recently, Africa (Ogle et al., 1979; Kawuki et al., 2003). Soybean rust was first observed in Uganda, Kenya, and Rwanda in 1996 and Zimbabwe in 1998 (Caldwell and Laing, 2001). Yield losses in commercial crops in Zimbabwe were 60-80%. The rust was thought to be wind-borne from Asia. Soybean rust was first observed in Nigeria in 1999 causing premature defoliation of infected plants (Akinsanmi et al., 2001). Seed weight reductions of 28-52% were also reported. Soybean rust first appeared in South Africa in March of 2001 causing yield losses ranging from 10-80%, with losses up to 100% in areas where soybean was grown continuously (Caldwell and Laing, 2001).

P. pachyrhizi was first detected in South America in February of 2001 in a limited number of fields in the Parana River Basin of Paraguay (Miles et al., 2003). By the next crop season in 2001-2002, rust was found on most soybean fields in Paraguay, but severe drought and fungicide usage helped to minimize crop losses (Yorinori et al., 2005). In Brazil, 60% of soybean acreage was infected by soybean rust. Yield losses were estimated to range from 30-75%, and total losses were estimated at $125.5 million ($220.50/t). The first report of soybean rust from Argentina occurred in 2002, and by 2003, rust was observed at most locations in Brazil south of the equator (Rossi, 2003; Yorinori et al., 2005). In Brazil that year, two fungicide sprays were applied to most fields at a cost of $592 million. Combined with yield losses estimated at over $1.5 billion, the total cost of soybean rust in Brazil surpassed $2 billion (Yorinori et al., 2005).

The United States leads the world in soybean production accounting for 40% of the total (Soy Stats, 2005). In 2004, 30.4 million hectares of soybeans were planted in the U.S. for uses including, but not limited to, soybean crush, soy meal production, livestock feed, soy oil production and consumption, edible fats and oils, and biodiesel fuel. Because of the heavy losses in South America, the USDA Economic Research Service (ERS) examined the possible economic and environmental impacts of soybean rust to the continental United States in April, 2004. The ERS study estimated that producer and associated domestic consumer losses in the United States could vary between $0.64 and $1.3 billion during the first year of establishment and $0.24 and $2.00 billion thereafter depending on the geographical extnt and severity of a rust epidemic (Livingston et al., 2004). After a

year of soybean rust establishment in the United States, the ERS has revised its potential loss estimates in 2005. Potential net profit losses for soybean producers were estimated to range between $0.393 and $1.688 billion annually, and total economic impacts on soybeans, other crops, and livestock producers were estimated to range from $0.586 and $1.862 billion annually (Johansson et al., 2005).

Soybean rust was first observed in the continental United States on November 6, 2004 in a field near Baton Rouge, Louisiana (Schneider et al., 2005). Analysis of the infected soybean plant tissue indicated that the rust was likely to have been present for 4 to 8 weeks. Isard et al. (2005) used historical weather data for each day in August and September of 2004 as input for an aerobiological modeling system, the Soybean Rust Aerobiology Prediction System (SRAPS). Output from the model showed that airflow patterns associated with Hurricane Ivan had the potential to transport spores from source regions in Colombia directly into the southeastern United States. The model showed that many spores released from the Rio Cauca source area in Colombia on 7, 8, 9 September could have remained viable while airborne until being deposited by precipitation in the southeastern United States between 15 and 18 September. The historical model output was given to members of the APHIS Soybean Rust Rapid Response team as a guide to field monitoring. In the months of November and December, many locations within 9 states in the southeastern United States were either confirmed to have soybean rust by using polymerase chain reaction (PCR) assays or had soybean rust like symptoms identified but not tested by PCR (Isard et al., 2005).

1.2 Resistance, Management, and the Soybean Rust Life and Disease Cycles

Two spore types have been found in nature for *P. pachyrhizi*: urediniospores and teliospores. The most common spore type is the urediniospore. The disease process begins when urediniospores are deposited onto a host (such as soybean or kudzu) and germinate. Once the urediniospores infect the host tissue, uredinia will begin to form after 5 to 8 days. At this point, more urediniospores can be produced, and continuous spore production can occur for up to 3 weeks. Infection is highly dependent on the microclimate within a host canopy. At least 6 hours of free moisture, or leaf wetness, is needed for infection. Ideally, 10-12 hours of leaf wetness and temperatures between 15 and 28 ºC are ideal for infection (Melching et al., 1989). Many spore cycles in the uredinial stage occur during a growing season, and the urediniospores are readily wind dispersed (Miles et al., 2005).

The presence of Asian soybean rust can be confirmed by viewing urediniospores under a microscope in the uredinial stage. Diagnosis has been based on visual observations of uredinia and urediniospores followed by confirmation by PCR (Melching et al., 1989; Harmon et al., 2006). Tan, red, and brown lesions develop on leaves and can be seen as early as four days after infection.

The telia and teliospores have also been observed on kudzu (*Pueraria lobata*) in central Florida and in soybean fields in Argentina (Harmon et al., 2006; Carmona et al., 2005). Under laboratory conditions, they have been germinated to produce basidiospores

(Saksirirat et al., 1991). No alternate host has been identified, therefore the life cycle has not been further characterized (Miles et al., 2005).

Very little is known about soybean host plant resistance to soybean rust (Hartman et al., 2005). Previously, four single genes were identified in four separate soybean plants for resistance to *P. pachyrhizi* isolates. These genes were all defeated in the field by other *P. pachyrhizi* isolates. Reports of partial resistance, such as reduced pustule number or increased latent period, exist in some soybean cultivars, but these cultivars have not been widely used in breeding programs. According to Hartman et al. (2005), the evaluation methods used in determining partial resistance and incorporating these methods into breeding programs is difficult and limited to use with older cultivars. To date, no commercial U.S. cultivars have been found to be resistant to *P. pachyrhizi* infection.

The best management strategy against soybean rust for the near future is the application of fungicides (Hartman et al., 2005). The timing of fungicide application is extremely important for soybean rust management efficacy. Research has shown that the first seasonal application of fungicides is the most important application, and the most appropriate timing of the application is in the early reproductive stages of the soybean crop when rust appears or is expected to appear in these early growth stages (Kemerait et al., 2005). The timing and necessity of fungicide usage is much better understood with advanced knowledge of the potential arrival of soybean rust. Spores that escape from a canopy can be dispersed locally within fields and to neighboring fields and long distances

up to several thousand kilometers. Their movement and timing are regular and predictable using an aerobiological modeling system (Isard et al., 2005).

1.3 Modeling and Previous Studies

Many passively moving organisms use the atmosphere as a medium of transport. The following are the stages of the aerobiological pathway: preconditioning in a source area, release and escape, horizontal transport, deposition, and impact in a destination area (Isard and Gage, 2001). Soybean rust urediniospores proceed through these stages (Isard et al., 2005). First, the spores are produced in an infected soybean field or on an alternative host. Weather variables, the growth stage of the soybean plant or alternative host, and the progress of the disease affect spore production. After spores are produced, wind, turbulence, location of the released spores within the canopy, and canopy structure are the primary variables that govern release and escape of spores from the canopy. Turbulent diffusion and wind shear dilute the spores that are transported by airflows, and weather variables such as ultraviolet radiation, temperature, and relative humidity affect the survival of spores in transport. Dry deposition by wind and turbulence and wet deposition by precipitation will deposit spores onto a destination area. If the destination area is a field of soybeans or an alternative host, various weather variables such as temperature and leaf wetness, and crop growth stage of the soybean field or alternative host can affect further disease development.

Many of the variables that govern the progress of soybean rust spores through the aerobiological transport process are well studied and understood (Isard et al., 2005). An important aspect of the modeling process for soybean rust spore movement through the atmosphere that is poorly understood is the escape of released spores from a canopy of soybeans. Many clouds of spores will escape a canopy and begin their local or long distance dispersal through the atmosphere, but most released spores will land on leaves or on the ground a short distance (less than a meter) from where they're produced within the canopy (Aylor, 1986). Only the spores that escape the canopy into the faster moving air above can contribute to the long distance spread of disease (Aylor and Ferrandino, 1985).

Although no empirical data exists for soybean rust urediniospore escape from a soybean canopy, estimates of spore escape do exist for similar spore types and crop systems. Aylor and Taylor (1983) estimated the escape rate of tobacco blue mold, *Peronospora tabacina*, spores from a diseased field of tobacco plants. They operated spore traps for 2-3 hours during times of expected peak spore release (900-1300 EST) at several heights above ground. Wind speed was measured at several heights above the canopy during periods when escape measurements were taken. They speculated that the escape of spores depended on turbulence and release rate. Additionally, even though maximum spore concentrations did not coincide with maximum release rates, they were closely correlated. The sedimentation rate due to gravity was assumed to be negligible as it reduced the upward flux of escaping spores by only 10%, and clumping of spores was either not taken into account or not observed for *P. tabacina*. They estimated the rate of spore escape to range from 1 to 7 per $m^{-2}s^{-1}$ (Aylor and Taylor, 1983).

Clumping of spores and sedimentation due to gravity were included in a later experiment conducted by Aylor and Ferrandino (1985). They estimated the escape of urediniospores of *Uromyces phaseoli* from a typical bean type canopy. Sedimentation due to gravity was included because it reduced escape rates by 20-30%. The gravitational settling speed was calculated for N clusters of urediniospores as $V_sN = 0.98\ V_{s1}N$^0.53. Ferrandino and Aylor (1984) previously calculated the settling speeds of clusters of spores and estimated the settling speed of a single urediniospore to be $V_{s1} = 0.0108$ m s^{-1}. The affect of clumping was also taken into account by counting singlets, doublets, triplets...and so on, separately. Escape of individual spore singlets was estimated to be 6-31 spores m^{-2} s^{-1}. This value was 2-7 times greater than that of doublets and 5-30 times greater than that of triplets. Relative concentrations of each agreed with the relative concentrations of numbers released within the canopy. The escape rate of spores and clumps of spores in this experiment increased with increasing turbulence. Since greater values of turbulence lead to greater spore dilution and the concentration of spores above the canopy increased rather than decreased with increasing turbulence, they speculated that more spores are released and escape as the canopy becomes more ventilated. A tendency for spore doublets and triplets also increased relative to singlets as turbulence increased, indicating that clusters of spores require more turbulence for release and escape than do singlets (Aylor and Ferrandino, 1985).

An assumption made by Aylor and Ferrandino (1985) will not likely hold: that the density of foliage was considered uniform with height does not apply to soybean plants

(Aylor and Ferrandino, 1985). The structure of a soybean canopy is not uniform with height, and preliminary data suggests that the structure changes dramatically over the course of a growing season. Figure 1.1 shows the cumulative proportion of leaf area at 6 dates during the 2005 growing season at a soybean field in Rock Springs, PA. Leaf area was calculated from volumes at height increments of 10.0 cm and an area of 0.5 x 0.5 m. Three samples were taken at each date and averaged. The profiles of leaf area did not increase linearly with height, and the proportion of leaf area found in the upper part of the soybean canopy increased as the season progressed. Figure 1.2 shows the cumulative proportion of leaf area at 5 dates during the 2006 growing season at a soybean field in Rock Springs, PA.

Figure **1.1**

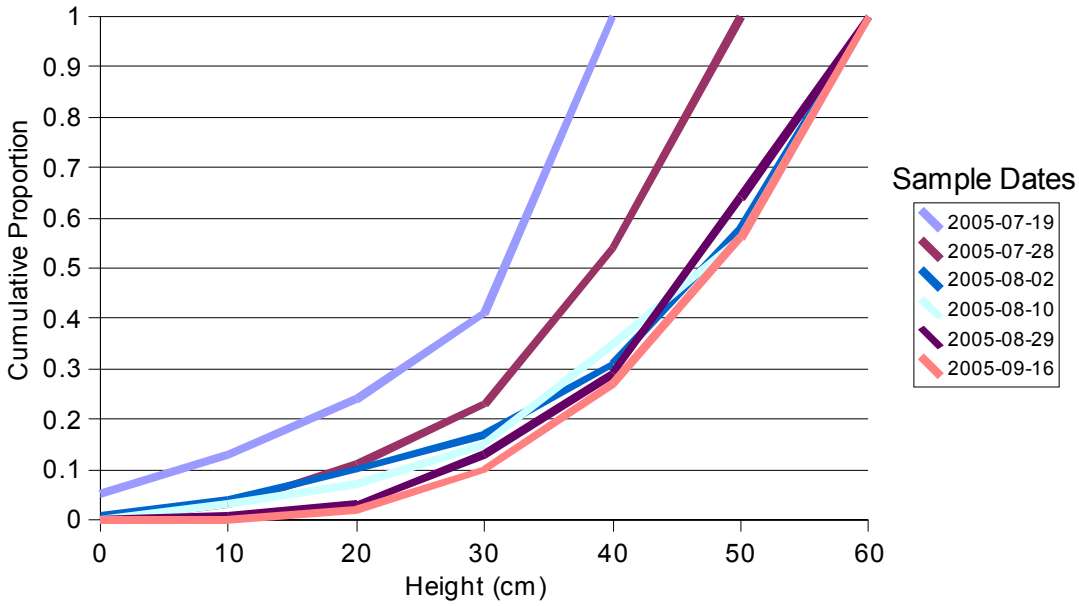

Fig. **1.1**: Cumulative proportions of leaf area in a soybean field at six dates during the 2005 growing season at Rock Springs, PA. Leaf area was estimated in volume slices at 10.0 cm increments of height and 0.5 x 0.5 m area at three locations.

Figure **1.2**

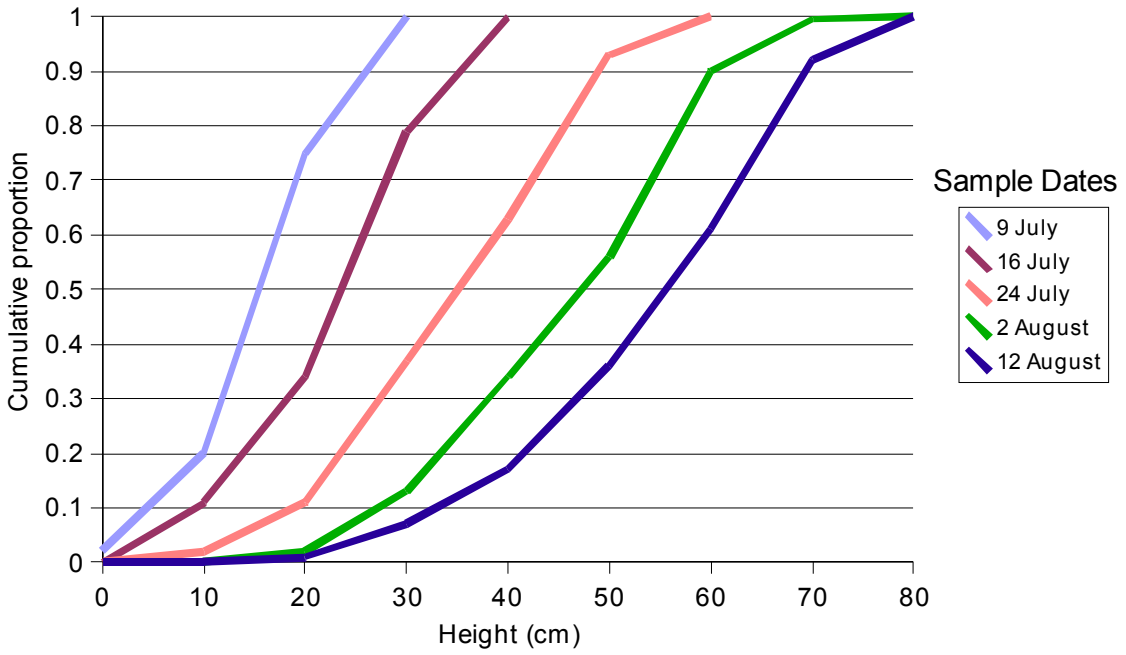

Fig. **1.2**: Cumulative proportions of leaf area in a soybean field at five dates during the 2006 growing season at Rock Springs, PA. Leaf area was estimated in volume slices at 10.0 cm increments of height and 0.5 x 0.5 m area at three locations.

1.4 Transport in the Turbulent Surface Layer of the Atmosphere

Atmospheric turbulence can be separated into two components: mechanical turbulence and thermal turbulence. Thermal turbulence is caused by incoming solar radiation heating the ground, which then heats the air. Consider a parcel of air at a certain temperature. If this parcel is displaced upward, in general one of three scenarios occurs: 1) the parcel is warmer than the surrounding air, 2) the parcel is of the same temperature as the

surrounding air, or 3) the parcel is colder than the surrounding air. Before proceeding further, it is important to define the term potential temperature (θ). Potential temperature is the temperature that an unsaturated parcel of dry air would have if brought adiabatically (no net energy gain or loss of the parcel, ie. no evaporation or condensation) from its original state to a standard pressure, usually 1000 mb. Potential temperature is conserved for all adiabatic processes. If the displaced parcel is in an environment that is colder than itself (using θ as the temperature measurements to account for changes of air pressure with height), it will continue to rise since its density is less than that of the surrounding air, and the layer of air in which the parcel will continue to rise before becoming negatively buoyant is considered to be unstable. If the parcel is at the same potential temperature as the surrounding environment the layer of air is considered to be neutrally stable. Finally, if the parcel of air is colder than the surrounding environment, any rising motion of the parcel will quickly slow, and the parcel will fall back to its original level. This condition is stable. As one considers deeper atmospheric layers (1000's of m), or allows for condensation and evaporation, the definitions for atmospheric stability must be modified to account for heat being added to or subtracted from the parcel of air. However, for the purposes of this research, considering stability to be driven by changes in potential temperature over the layer above the surface in question (the surface layer or constant flux layer in the lowest 100 m or so of the atmosphere), any temperature differences will only be on the order of 0.1 °C.

Mechanical turbulence is caused by obstructions to wind flow. In the free atmosphere (no friction opposing the wind flow), wind direction and speed are determined by a balance

of forces between the pressure gradient force and the Coriolis force. This type of wind flow, referred to as geostrophic wind, typically occurs far above the surface (> 1.0 km). As one proceeds toward the surface, the wind becomes obstructed and slowed by features such as mountains and even the type of surface cover (ie. water, forest, open grassland), and closer to the surface buildings, trees, and crops. This friction with the earth's surface elements creates drag which slows air movement. This drag force per unit ground area has dimensions of force per unit area. These dimensions are equivalent to density (in this case the density of the moving air) multiplied by velocity squared (ρu^2). This velocity is referred to as the friction velocity (u^*) which is a reference velocity indicating the rate at which momentum is transferred to the surface. The product of the two represents the shearing stress (often called Reynold's stresses) on the moving air. Picture air moving over the surface of the earth. Friction is exerted on the moving air resulting in the air being slowed at different rates with height (the force of friction is felt more as one proceeds toward the earth's surface). As a consequence, the air to piles up and overturns on itself, which in turn causes turbulent eddies. The strength of the frictional force, as well as the strength of the forces determining the speed of the moving air, will determine the size and strength of the turbulent eddies. Therefore, the stronger the wind speed, the greater the mechanical turbulence. As the wind speed diminishes, mechanical turbulence is also diminished. If no thermal turbulence caused by convection exists, the airflow is said to be laminar. In the planetary boundary layer (typically the lowest 100 m to 2.0 km of the atmosphere) the atmosphere is considered to be completely and continuously turbulent. Nearly all air motion is turbulent, and the mixing of properties (CO_2, water vapor, momentum, spores, air pollutants) depends on turbulence (Woodward and Shealy,

1983 and Webb, 1965). Laminar layers in nature typically exist only in the lowest few millimeters (Lowry and Lowry, 1989) and are not important when considering a surface layer many meters deep.

Turbulent fluxes can be evaluated directly by the eddy covariance method (Webb, 1965). Wind speed varies in an irregular pattern, making it different from other motions like waves. Turbulence, however, is not completely random because over a time period of minutes to an hour or so, generally a statistically-stable mean value for wind speed can be found. In general, turbulent fluctuations vary in size and frequency with smaller eddies occurring much more frequently than larger eddies. The spectrum of turbulence peaks at three time periods. The peak near 100 hours is wind speed variations associated with frontal passages and other synoptic scale weather variations. The peak at roughly 24 hours is the diurnal variation in wind speed, and the peak around 0.1 to 0.01 hours results from turbulent fluctuations due to thermal and mechanical turbulence. Between the peak at 24 hours and the peak at 0.1 to 0.01 hours is a period ranging from roughly 10 minutes to 2 hours with little variation in wind speed. This period is referred to as the spectral gap between variations of the mean flow (hours to days) and turbulence (seconds to minutes) (Stull, 1988). It is within this spectral gap that the measurement period of 15 minutes for each trial was chosen.

The wind can be separated into two components, the mean wind plus any deviation from the mean wind. Mean wind can be expressed as:

$$S = [S] + S'$$

where [S] is the average wind speed and S' is the instantaneous deviation from the mean wind speed. By measuring over time periods within the spectral gap, [S] is virtually constant over that time period compared to longer time periods, and S' is the turbulent portion of the total wind speed S at any given moment in time. A fast-response instrument must be used to generate a time series of means and deviations that can be statistically analyzed (roughly 10 measurements per second for the entire time period of the trial). Once the time series have been created, multiplying the deviations together as a covariance (for example, w'S' for the transport of horizontal wind speed in the vertical) and taking the average of these covariances yields the estimate of the turbulent fluxes (Stull, 1988 and Lowry and Lowry, 1989). Some examples of these fluxes are (again using [ ] as the averaging function):

$$\text{Momentum} = \rho[w'S']$$

$$\text{Heat} = \rho c_p[w'\theta']$$

$$\text{Water vapor} = \rho[w'q']$$

$$\text{Carbon dioxide} = \rho[w'c'].$$

A second approach to estimating turbulent fluxes (F) is the aerodynamic method (Lowry and Lowry, 1989). One such approach estimates from mean quantities (such as water vapor, spore concentrations, carbon dioxide) measured at two or more heights above the surface and depends on flux-profile relationships (Webb, 1965). If the turbulence is fully

developed so that the friction velocity equals the downwind and crosswind velocities (u* = u = w), then the flux of a substance through the layer can be estimated by knowing the wind speed S and the concentration of the substance at known upper and lower measurement levels (Lowry and Lowry, 1989). The flux estimate for momentum (F), for example, is

Equation **1.1**

$$F = -[\rho]K_M(z)(d[u]/dz) \qquad \text{Eq. } \mathbf{1.1}$$

where K_M is the diffusivity of momentum. Using the relationship $d[u]/dz = u^*/\{k(z-D)\}$, the flux estimate for momentum becomes

Equation **1.2**

$$F = -[\rho]K_M(z)u^*/\{k(z-D)\} \qquad \text{Eq. } \mathbf{1.2}$$

where k is the von Karmen constant (shown experimentally to be 0.4) and D is the zero-plane displacement height. This method requires the assumption of neutral stability which makes the profiles of wind speed and the concentration of the flux logarithmic (Woodward and Shealy, 1983).

Assuming a flux F, the flux-gradient method states that F = A (dC/dz), where A is the exchange coefficient (*austausch coefficient*) and C is the concentration of F (per unit mass) of air. Since flux is related to both the density of air and how developed the turbulence is, $A = \rho K$ so $F = \rho K(dC/dz)$. Conceptually, the exchange coefficient A plays the same role and has the same units as thermal diffusivity, but is much more variable with height, wind speed, and time of day. Varying wind speed from 1 to 10 m s^{-1} will

vary the exchange coefficient by 2 orders of magnitude at night, and as much as 30-100 g cm^{-1} s^{-1} during the daytime (Lowry and Lowry, 1989).

An assumption of note in estimating fluxes from profiles is that the boundary layer is neutrally stable. In order to account for buoyant forcing in these types of flux estimates, an account must be taken of how the eddy diffusivity K responds to changes in stability. The Richardson number (Ri) is the ratio of the rate of buoyant consumption of turbulence to the rate of mechanical production of turbulence. Many derivations and types of Ri exist, but all essentially deal with this ratio. The effect on K_M is as follows: as stability increases ($Ri > 0$), K_M gets smaller at a gradual rate, and as stability decreases ($Ri < 0$), K_M gets larger rapidly. Eddy diffusivity for other properties other than momentum respond more to changes in stability (Lowry and Lowry, 1989 and Webb, 1965). The Richardson number, then, is used as a correction factor for estimating fluxes from concentration profiles. A major disadvantage of using the Richardson number is that it must be calculated at each measurement height (Woodward and Shealy, 1983). Monin and Obukhov defined stability in terms of a scale height representing an expansion or contraction of the turbulent boundary layer. The Monin-Obukhov stability parameter is considered to have a stronger theoretical basis than the Richardson number and was used in the analysis of this research (Rosenburg et al., 1983). For a full derivation, see Appendix A.

The heat budget method is used to estimate heat fluxes and is valid over land and water. Over land, this method makes use of the heat budget (neglecting photosynthesis) in which

the incoming radiation minus the radiation that goes through the ground balances the sum total of the sensible heat flux and the latent heat flux. By making use of the Bowen ratio, the ratio of the sensible heat flux to the latent heat flux, and assuming the diffusivities of latent heat and sensible heat are equal, the fluxes can be estimated by measuring the changes of potential temperature and specific humidity with height (Webb, 1965).

1.5 Objectives

The aerial movement and timing of the transport of *P. pachyrhizi* spores are regular and predictable using an aerobiological modeling system (Isard et al. 2005). Many of the variables that govern the progress of spores through the aerobiological transport process are well studied and understood. An important part of the modeling process for soybean rust spore movement through the atmosphere that is poorly understood is the escape of released uredineospores from a canopy of soybeans (Isard et al 2005).

The objectives of this research were to: 1) quantify the proportion of released soybean rust spores and particles that escape a soybean canopy throughout the growing season and relate this value to turbulence and canopy structure, 2) create concentration profiles of spores and particles and estimate vertical fluxes out of the canopy, and 3) provide a descriptive assessment of the directional and spatial components of movement for spores and particles in and above the canopy. The findings from this research will enhance our

ability to predict the movement of soybean rust and more accurately predict where epidemics may occur.

Chapter 2

Methods

P. pachyrhizi urediniospore escape was estimated as part of three separate experiments in soybean canopies. The first experiment was a simulation of urediniospore (referred to as "spore" hereafter) escape from a soybean canopy using DayGlo® (DayGlo Color Corp., Cleveland, OH) paint chip particles. The second experiment was a series of field trials designed to monitor spore escape in a field of soybeans infected with Asian soybean rust. The third experiment was a series of field trials designed to monitor the escape of spores released from the center of a field free of *P. pachyrhizi*. During the second and third experiments, spore simulation trials with paint chip particles were conducted simultaneously with trials where actual spores were collected.

2.1 Particle Escape Experiment

An experiment (PAp) consisting of 16 trials were conducted on the Russel E. Larson Agricultural Research Farm at Rock Spring, PA (10 July 2006 – 11 August 2006) and in two separate fields located at the University of Florida, North Florida Research and Education Center in Quincy, FL (22 August 2006 – 28 August 2006, 27 September 2006

– 2 October 2006). Row spacing treatments were 38.1 cm (15.0 in) for the field in PA and 17.78 cm (7.0 in) and 76.2 cm (30.0 in) for the two fields in FL. Time of day at which the trials were conducted is shown in Table 2.1, and growth stages ranged from early vegetative to late reproductive growth stages.

DayGlo NG-20 paint chips were used to simulate soybean rust spores. The paint chips have a median particle size of 20.0 μm. For each simulation, 10.0 g, or roughly 133 billion particles, were sifted through a 50.0 μm U.S. Standard Sieve (Fisher Scientific Co., Hampton, NH) onto the soybean canopy. The particles were collected by rotorod impaction samplers. Each rotorod's rotation rate was calibrated in rpm using a tachometer at the end of the season. Each rotorod sampler contained two rods and spun clockwise. The rods had silicon grease on the face that spun into the wind.

2.2 Spore Escape Experiments

The first spore escape experiment (FLCs and FLCp; the ‘s’ and ‘p’ refer to trials during the experiment where spores or particles were released) was conducted at the University of Florida, North Florida Research and Education Center in Quincy, FL (22 August 2006 – 28 August 2006). The field was one of the more mature sentinel plots and was assumed to be uniformly infected with *P. pachyrhizi*. Row spacing in the field was 17.78 cm (7.0 in), and the canopy was closed. The soybeans were in late reproductive growth stages.

Spores were allowed to release naturally in ambient environmental conditions and were collected in the same manner as the particles in the previous experiment. A total of 12 trials were conducted at times shown in Table 2.2. Particle escape trials were run simultaneously (see Table 2.1).

The second spore escape experiment (FLOs and FLOp) was conducted again in Quincy, FL (27 September 2006 – 2 October 2006). Three control trials were run to assure the field showed no symptoms of being infected with *P. pachyrhizi*. Row spacing in the field was 76.2 cm (30.0 in), and the canopy was open. The soybeans were in the late vegetative to early reproductive stages. Spores were released and collected in the same manner as the particles in the particle escape experiment, but only 0.5 g of spores were sifted onto the soybean canopy. A total of 7 trials were conducted along with 3 additional control trials (two prior to and one after the experimental period) at times shown in Table 2.2. Particle escape trials were run simultaneously to the spore escape trials and were also included in the control trials (see Table 2.1).

2.3 Meteorological Instrumentation

Meteorological conditions were measured by a 3-dimensional sonic anemometer (CSAT3) (Campbell Scientific, Inc., Logan, UT), a Vaisala Temperature/RH probe (HMP45C) (Vaisala, Inc., Vantaa, Finland), and an R. M. Young Wind Sentry Set

(03001-L) containing a wind vane and cup anemometer (Campbell Scientific, Inc., Logan, UT). The CSAT3 and 03001-L measured wind speed and direction, and the HMP45C measured relative humidity and air temperature. The CSAT3 also measured air temperature (Table 2.3). These measurements were used to estimate turbulence and provide back ground meteorological data. Meteorological measurements made by the CSAT3, 03001-L, and the HMP45C were recorded and stored by a CR23X data logger (Campbell Scientific, Inc., Logan, UT).

2.4 Canopy Structure Measurements

Canopy structure was estimated by removing leaves from soybean plants at specific heights and estimating leaf area. Leaves were cut from a volume whose length and width are 0.5 m. The leaves were cut at height increments of 10.0 cm from the ground to the top of the canopy with the number of levels depending on the height of the canopy. The cut leaves were placed in sealed plastic bags labeled according to height in the canopy. Next the leaves were scanned to create a digital image in Tagged Image File Format (TIFF). Finally, leaf area at each 10.0 cm height increment was estimated by a computer program.

The computer program was written in C and uses the library 'tiffio.h' to interpret the TIFF files. The program changed each pixel in the TIFF image of leaves to gray scale and

sorted each pixel into white or non-white categories. The number of non-white pixels were counted for each image and divided by the total number of pixels per cm^2. The resulting value was the total leaf are in cm^2 shown in the TIFF image. From this value, leaf area index (LAI) was calculated at each height increment by dividing the total leaf area by the total ground area (2500 cm^2).

2.5 Meteorological and Collection Instrument Location

The rotorods were placed on vertical towers at heights determined by the height of the canopy, h, in cm. The rotorods were located at the following heights on the towers: 0.5 h, 1.0 h, 1.5 h, and 2.5 h (see Figure 2.1). Four vertical towers were situated in the soybean field in a square (3.0 x 3.0 m) close to the center of the soybean field to minimize the amount of airborne spores originating from other infected soybean fields for the spore collection experiments. Both particles and spores collected with rotorods were assumed to have originated from the target soybean field only. The location of the CSAT3 was between 2.0-3.0 m away from the square collection grid, and the height of the anemometer was 1.0 m above the canopy height (h + 1.0 m). Figures 2.2 and 2.3 show the locations of the collection and meteorological instruments.

2.6 Collection and Measurement Duration

At the beginning of each trial, if sifting was necessary, spores and/or particles were sifted onto the soybean canopy in the center of the collection grid at 0.5 h. After sifting, the rotorod samplers were started and remained spinning for 15 minutes. During the sampling period, the CSAT3 measured u (downwind), v (crosswind), and w (vertical) components of wind velocity (m s^{-1}) and air temperature T_a (°C) at 10.0 Hz, and the HMP45C measured relative humidity RH (%) and T_a at one minute increments. These data were recorded by the CR23X and averages and covariances were calculated at varying intervals as shown in Table 2.4. At the conclusion of each trial, the rotorod slides were packaged in plastic containers and refrigerated. Particles and/or spores on each rod were then counted under 100X magnification to determine the total count of each. The volume of air sampled during each trial, V, in m^3 is given by the equation

Equation **2.1**

$$V = W\lambda d\pi\sigma t \qquad \text{Eq. } \mathbf{2.1}$$

where W is the rod width in m, λ is the rod length in m, d is the head diameter in m, σ is the number of rotorod revolutions per minute (min^{-1}), and t is the time in minutes. After estimating the volume of air sampled, the concentration per rotorod in spores or particles per m^3, C, was estimated by

Equation **2.2**

$$C = p / V \qquad \text{Eq. } \mathbf{2.2}$$

where p is the total count of spores or particles. Canopy structure measurements were carried out roughly once per week during the experimental trial periods. Each trial was assigned a canopy structure value estimated on the date of the trial, or the value was interpolated from the two closest canopy structure estimates.

2.7 Analysis Methods

The analysis for all experiments involved a qualitative comparison of the spatial distribution of airborne concentrations of spores (or particles) to meteorological variables and a quantitative comparison of airborne concentrations of spores (or particles) to meteorological and canopy structure measurements using multivariate linear regression. An ANCOVA test was performed on the substance (spore or particle) and canopy type (open and closed) during the two experiments conducted in Florida to assess any difference in behavior between spores and particles in different canopy types. Finally, vertical fluxes of spores and particles leaving the canopy were estimated from concentration profiles.

Figure **2.1**

Fig. **2.1**: The location of the rotorods on the tower relative to the height of the canopy h. Concentration profiles can be estimated by collecting spores or particles with rotorods located at each height on a tower.

Table **2.1**

Tab. **2.1**: The date, time of day, canopy height, and canopy closure for the particle escape experiment. During trial FL2-10, many rotorod slides were damaged, therefore this trial was not used in the final analysis.

Trial	Date	Time of Day (LST)	Canopy Height (cm)	Canopy Closure
PA1	07/10/06	1200	35	open
PA2	07/13/06	1000	48	open
PA3	07/13/06	1200	48	open
PA4	07/13/06	1400	48	open
PA5	07/24/06	1000	65	closed
PA6	07/24/06	1200	65	closed
PA7	07/24/06	1400	65	closed
PA8	08/02/06	1000	80	closed
PA9	08/02/06	1200	80	closed
PA10	08/02/06	1400	80	closed
PA11	08/09/06	1000	80	closed
PA12	08/09/06	1200	80	closed
PA13	08/09/06	1400	80	closed
PA14	08/11/06	1000	80	closed
PA15	08/11/06	1200	80	closed
PA16	08/11/06	1400	80	closed
FL1	08/22/06	1000	100	closed
FL2	08/22/06	1200	100	closed
FL3	08/22/06	1400	100	closed
FL4	08/23/06	1100	100	closed
FL5	08/23/06	1337	100	closed
FL6	08/24/06	1200	100	closed
FL7	08/25/06	1000	100	closed
FL8	08/27/06	1330	100	closed
FL9	08/27/06	1615	100	closed
FL10	08/28/06	1220	100	closed
FL11	08/28/06	1400	100	closed
FL12	08/28/06	1600	100	closed
FL2-1	09/27/06	1000	60	open
FL2-2	09/27/06	1400	60	open
FL2-3	09/28/06	1400	60	open
FL2-4	09/29/06	1200	60	open
FL2-5	09/29/06	1400	60	open
FL2-6	09/30/06	1000	70	open
FL2-7	09/30/06	1200	70	open
FL2-8	09/30/06	1400	70	open
FL2-9	10/02/06	1000	70	open
FL2-10	10/02/06	1400	70	open

Table **2.2**

Tab. **2.2**: The date, time of day, canopy height, and canopy closure for the spore escape experiments. During trial FL2-10, many rotorod slides were damaged, therefore this trial was not used in the final analysis for the particles. Of the rotorod slides that could be salvaged, spores were not seen.

Trial	Date	Time of Day (LST)	Canopy Height (cm)	Canopy Closure
FL1	08/22/06	1000	100	closed
FL2	08/22/06	1200	100	closed
FL3	08/22/06	1400	100	closed
FL4	08/23/06	1100	100	closed
FL5	08/23/06	1337	100	closed
FL6	08/24/06	1200	100	closed
FL7	08/25/06	1000	100	closed
FL8	08/27/06	1330	100	closed
FL9	08/27/06	1615	100	closed
FL10	08/28/06	1220	100	closed
FL11	08/28/06	1400	100	closed
FL12	08/28/06	1600	100	closed

Trial	Date	Time of Day (LST)	Canopy Height (cm)	Canopy Closure
FL2-1*	09/27/06	1000	60	open
FL2-2*	09/27/06	1400	60	open
FL2-3	09/28/06	1400	60	open
FL2-4	09/29/06	1200	60	open
FL2-5	09/29/06	1400	60	open
FL2-6	09/30/06	1000	70	open
FL2-7	09/30/06	1200	70	open
FL2-8	09/30/06	1400	70	open
FL2-9	10/02/06	1000	70	open
FL2-10*	10/02/06	1400	70	open

* denotes a control experiment where no spores were sifted onto the canopy

Table **2.3**

Tab. **2.3**: Meteorological variables measured during field trials. Measurements from the CSAT3 were used in calculations, while all other measurements were used as back ground data. (u = downwind velocity vector, v = crosswind velocity vector, w = vertical velocity vector, Ta = air temperature, RH = relative humidity, wdr = wind direction, wsp = wind speed).

Variable	Device	Operating Range (°C)	Measurement Range	Period	Error (+/-)
u (m s^{-1})	CSAT3	-30 – 50	+/- 65.536 m s^{-1}	10 Hz	4.0 cm s^{-1}
v (m s^{-1})	CSAT3	-30 – 50	+/- 65.536 m s^{-1}	10 Hz	4.0 cm s^{-1}
w (m s^{-1})	CSAT3	-30 – 50	+/- 65.536 m s^{-1}	10 Hz	4.0 cm s^{-1}
Ta (°C)	CSAT3	-30 – 50		10 Hz	
Ta (°C)	HMP45C	-40 – 60		1.0 min	
RH (%)	HMP45C	-40 – 60	10 – 100 %	1.0 min	2 (10-90 %), 3 (90-100%)
wdr (deg)	03001-L			1.0 min	
wsp (m s^{-1})	03001-L			1.0 min	

Table **2.4**

Tab. **2.4**: Calculations from meteorological measurements used in the data analysis. S is the horizontal wind speed, and Ts is the sonic virtual temperature. The two covariance calculations were used to estimate mechanical and thermal turbulence (see chapter on spore escape analysis).

Calculation	Operating Range (°C)	Period	Error (%)
average u	-25 – 50	1.0 min	0.01
average v	-25 – 50	1.0 min	0.01
average w	-25 – 50	1.0 min	0.01
average S	-25 – 50	1.0 min	0.01
cov(w'Ts')	-25 – 50	1.0 min	0.01
cov(w'S')	-25 – 50	1.0 min	0.01

Figure **2.2**

Fig. **2.2**: Location of meteorological and collection instruments during a particle escape trial in Rock Springs, PA. A similar design was used for each of the three experiments.

Figure **2.3**

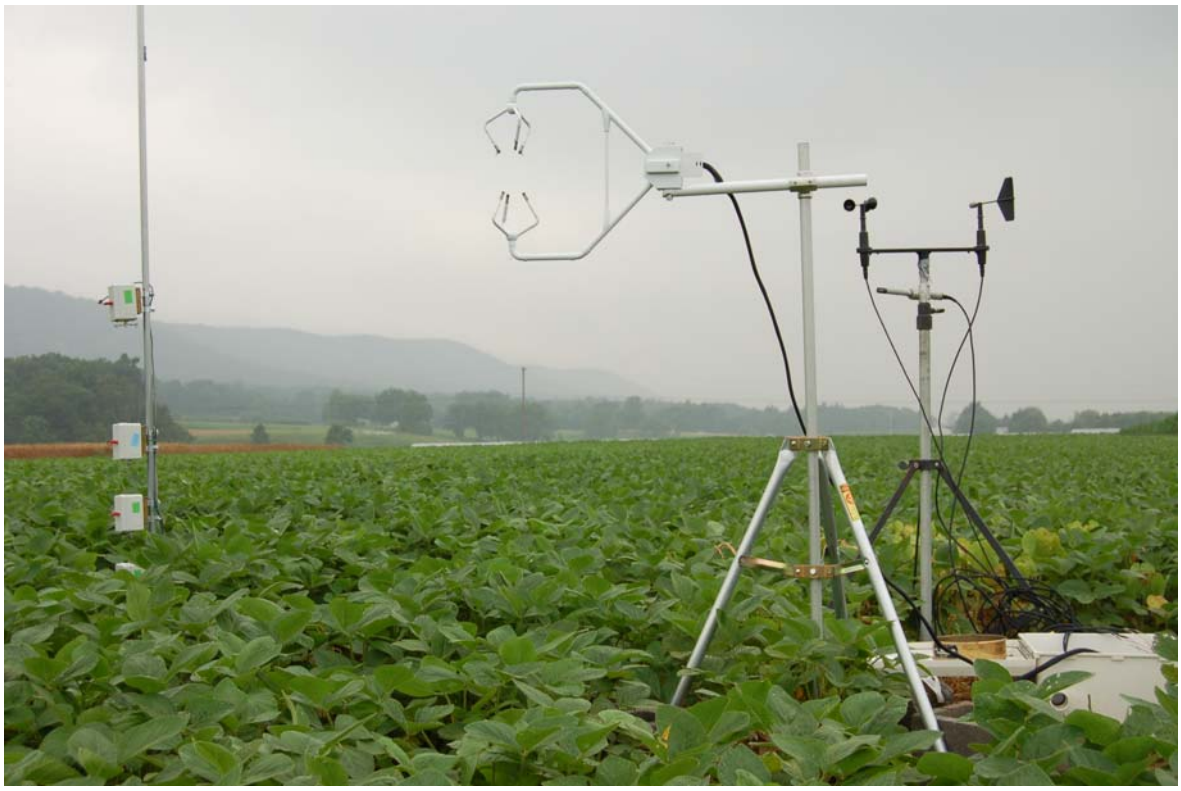

Fig. **2.3**: Close up view of the CSAT3 and 03001-L. TheCR23X data logger was stored in a white box on the ground between the two instruments. Also shown in this image is the HMP45C.

Chapter 3

Analysis: Spore and Particle Escape from a Soybean Canopy

The first objective of this research was to quantify the proportion of released soybean rust spores and particles that escape a soybean canopy throughout the growing season and relate that value to environmental variables, such as turbulence, and canopy

structure. Multivariate linear regression models were chosen to explain the relationship of spore or particle escape to environmental variables. The predictor variables for regression models were chosen based on the Mallows C-P best subsets test and based on predictor variables that were consistently strong for trials using particles and spores as well as trials conducted in open canopy and closed canopy soybean fields. The predictor variables chosen were H, s, LAI, T, s*LAI, and T*LAI where H is the rotorod height (m), s is the Monin-Obukhov stability parameter (see Appendix A), T is mechanical turbulence expressed as the maximum value of the covariance of w (vertical wind speed in m s^{-1}) and S (horizontal wind speed in m s^{-1}), and LAI is the total leaf area index above 0.5 h, the release level in the canopy. For interaction terms, each term was centered before being added to the regression model. The continuous predictor variables were centered by subtracting the mean value of the predictor variable from each predictor value. By centering a term, many of the problems with multicollinearity, correlated predictor variables explaining the same variability, were avoided.

3.1 Spores

Escape of spores, Y, was determined by dividing the estimate of spore concentration at 1.5 h by the estimate of spore concentration at 0.5 h on the same tower. During the closed canopy Florida trials, each tower was included in the analysis since the field was uniformly diseased. During the open canopy Florida trials, only measurements

from the tower that had the highest spore concentration in its profile were used in the analysis. If another tower from the same trial had a profile with concentrations of the same order of magnitude, it was also included in the analysis. The escape percent in the open canopy Florida trials can be expressed as

Equation **3.1**

$$Y' = 2.10 - 0.120\ H - 0.0638\ T + 0.163\ s \qquad \text{Eq. } \mathbf{3.1}$$

(R-squared 90.6%, p = 0.048) where $Y' = 2 * \arcsin(\sqrt{Y})$ (see Appendix C for a graphical interpretation and description of transformation). LAI as an independent predictor variable was not included in this equation as LAI remained unchanged during the open canopy Florida trial period. Figure 3.1 shows the profile of LAI.

Leaf area did change during the closed canopy Florida trials, and the escape percent can be expressed as

Equation **3.2**

$$Y' = 4.44 + 0.224\ T - 0.007\ LAI + 0.200\ s - 0.314\ LAI*s - 0.356\ LAI*T \qquad \text{Eq. } \mathbf{3.2}$$

(R-squared 77.8%, p = 0.055). H did not change during the experiment as the canopy had finished growing. Figure 3.2 shows an example of an LAI profile during the closed canopy Florida experiment. LAI ranged from 4.49 to 4.77. Although the p-value is not significant ($\alpha = 0.05$), its value is quite low.

3.2 Particles

Escape of particles was determined by dividing the estimate of particle concentration at 1.5 h by the estimate of particle concentration at 0.5 h on the same tower. Towers used in the analysis (open and closed canopy) were determined using the same process as the open canopy spore experiment. The Pennsylvania particle escape trials were conducted from July 9, 2006 to August 12, 2006. The canopy grew from 35.0 cm to a maximum height of 80.0 cm during the time period. Figures 3.3 and 3.4 show an early and late season graph of LAI respectively, and Figure 3.5 shows the progression of LAI throughout the experiment as a cumulative percent with height within the canopy. During the experiment, LAI ranged from 2.03 on 9 July 2006 to 7.03 on 8 August 2006.

Figure **3.1**

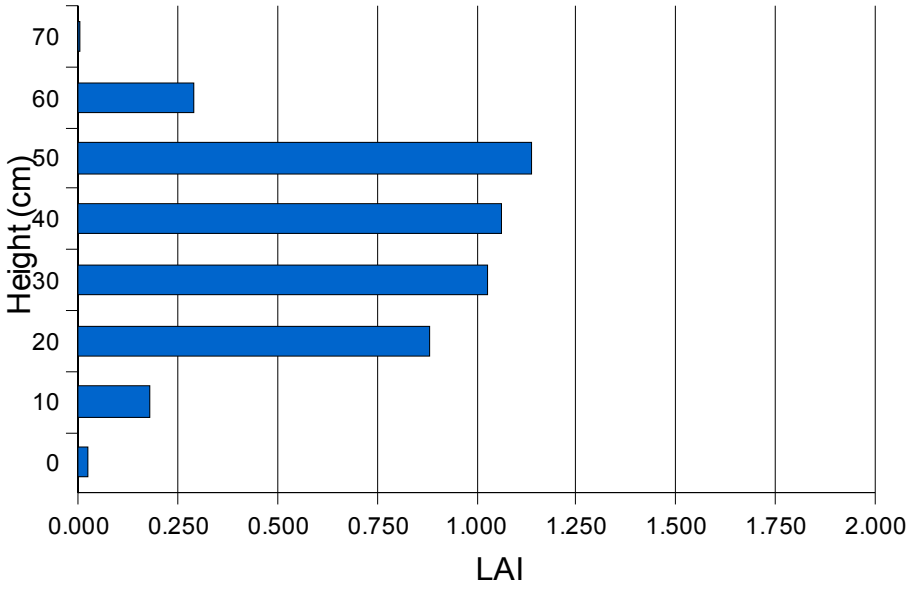

Fig. **3.1**: Leaf area index (LAI) at various heights within an open canopy in Florida. Canopy height was 75.0 cm. Total LAI was 4.61.

Figure **3.2**

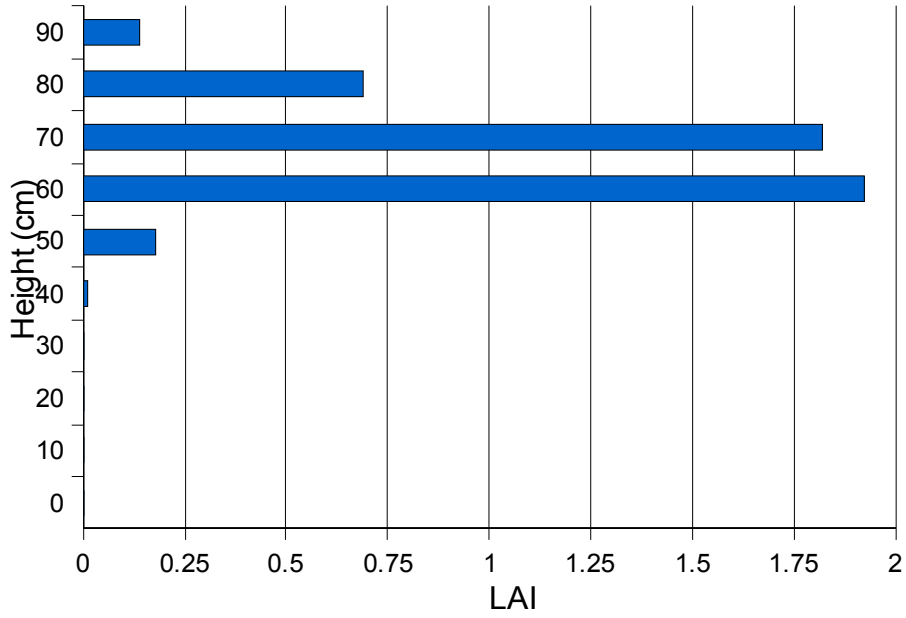

Fig. **3.2**: Leaf area index (LAI) at various heights in a closed canopy taken on 23 August 2006 in Florida. Canopy height was 100.0 cm. Total LAI was 4.77.

The best model for expressing particle escape percent for open canopy trials was Equation **3.3**

$$Y' = -4.00 - 0.0209\ H - 0.0661\ T + 2.53\ LAI \qquad \text{Eq. } \mathbf{3.3}$$

(R-squared 79.4%, $p < 0.05$). This expression explained both the Pennsylvania and Florida open canopy particle trials. Figure 1 shows the LAI profile for the Florida open canopy trials. Using a model that contains all of the variables from Equations 3.1 and 3.2 increases the R-squared value, but the variance inflation factors (VIF) were quite large (> 100 for T, s, LAI*s, and LAI*T). The VIF is a measure that estimates how much

the variance of an estimated coefficient increases based on correlation of predictor variables. The model including all of the parameters was

Equation **3.4**

$$Y' = 8.3 - 0.27\,H + 0.144\,T - 1.43\,LAI + 1.09\,s + 0.68\,LAI*s + 0.128\,LAI*T \quad \text{Eq. } \mathbf{3.4}$$

(R-squared 81.3%, $p < 0.05$).

Figure **3.3**

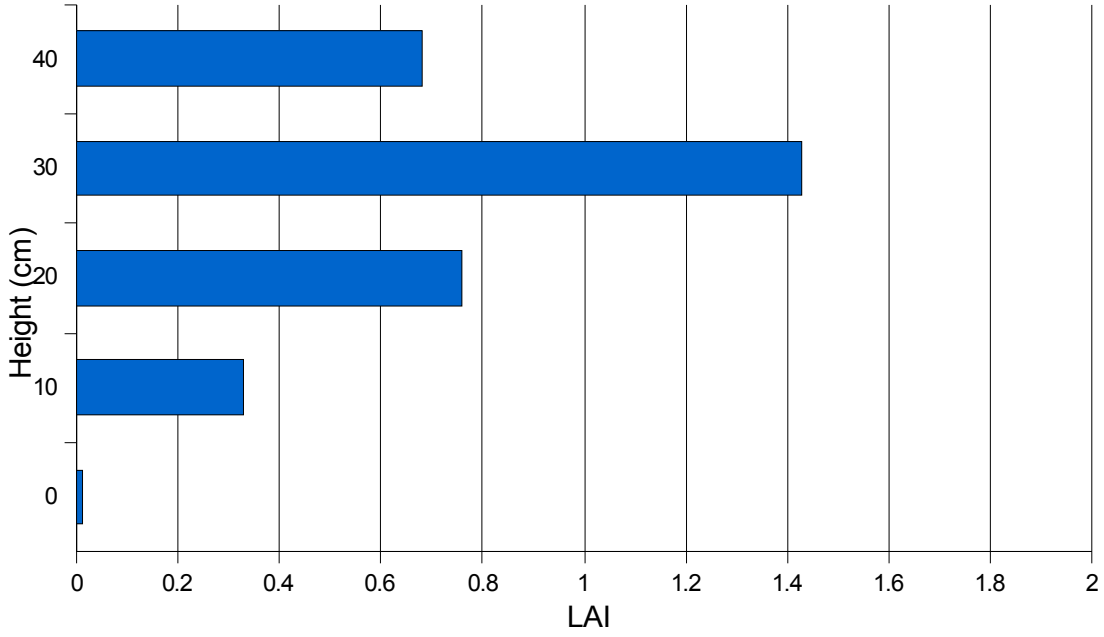

Fig. **3.3**: Leaf area index (LAI) at various heights within the soybean canopy taken on 16 July 2006 in Pennsylvania. The canopy height was 48.0 cm. Total LAI was 3.22.

Figure **3.4**

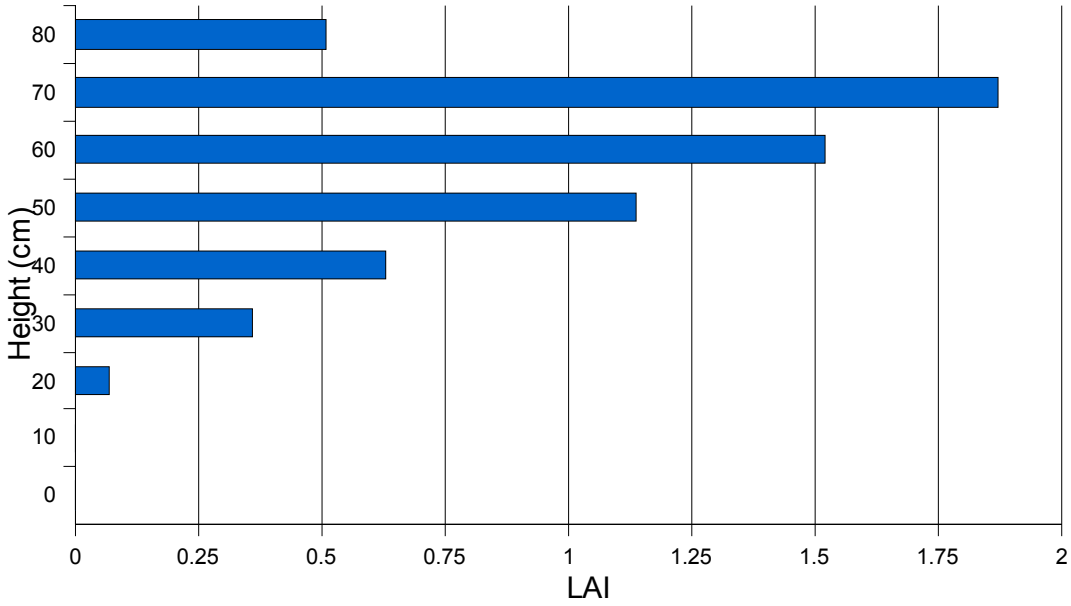

Fig. **3.4**: Leaf area index (LAI) at various heights within the soybean canopy on 12 August 2006 in Pennsylvania. The canopy height was 80.0 cm. Total LAI was 6.09.

Figure **3.5**

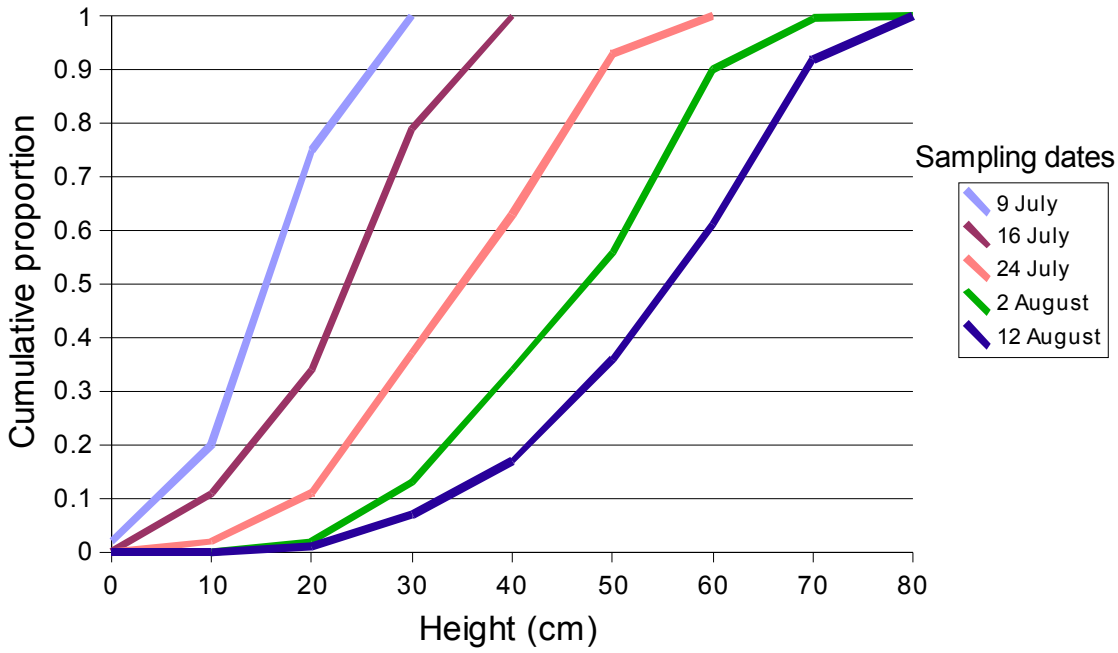

Fig. **3.5**: Leaf area index (LAI) profiles throughout the experiment period (9 July 2006 to 12 August 2006) in Pennsylvania.

No satisfactory relationship was found for the closed canopy particles in the Florida experiment, the Pennsylvania experiment, or for the results pooled over both sites. While the spores in the closed canopy trials were released in quantities throughout the canopy relative to the amount of leaf area, the particles were only released at one level, 0.5 h. It was apparent that other processes were contributing to the concentration of particles in the lower canopy, thus affecting the proportion of particles that escape. After the canopy closed and as the season progressed, LAI decreased in the lower parts of the canopy due to leaf senescence of older leaves at lower positions in the canopy. In the Pennsylvania experiment the lower canopy became more ventilated for wind flow, and

fewer leaves were present to obstruct within canopy movement of spores. Therefore, a greater concentration of particles was found in the lowest part of the canopy when spores were released in a closed canopy. This was true despite the meteorological conditions being similar and the number of particles sifted onto the canopy being equal.

3.3 Combining Model Results

Trials conducted in open canopies using either spores or particles were combined to produce one regression model. Using all of the predictor variables, the model fit well (R-squared 84.1%, $p < 0.05$), but the stability parameter s and its interaction with leaf area inflated the variance. The best model for the open canopy was

Equation **3.5**

$$Y' = -4.18 - 0.02\ H - 0.0784\ T + 2.59\ LAI - 0.181\ Substance \qquad \text{Eq. } \mathbf{3.5}$$

where the substance term is a categorical indicator for the type of substance used in the trial (0 = spores, 1 = particles) (R-squared 81.8%, $p < 0.05$). No satisfactory results could be found for the combination of all closed canopy trials.

To combine all of the data together in one model, the first step was to include all data for which valid regression models could explain variability (all spore trials and open canopy particle trials). Several models fit this condition well, but the model with the best fit and the least variation inflation factors was

Equation **3.6**

$$Y' = -0.284 + 0.324\ LAI + 0.0924\ s - 0.147\ LAI*s \qquad \text{Eq. } \mathbf{3.6}$$

(R-squared 67.2%, $p < 0.05$).

The next step is to add the data for which no satisfactory relationship could be found. The best relationship explaining all trials regardless of substance, release type, and canopy type was

Equation **3.7**

$$Y' = 0.209 - 0.0764\ T + 0.549\ canopy + 0.0882\ T*\ canopy \qquad \text{Eq. } \mathbf{3.7}$$

(R-squared 48.6%, $p < 0.05$). The term 'canopy' represents a categorical variable to indicate whether the canopy was open or closed (0 = open, 1 = closed).

3.4 Particles versus Spores

An ANCOVA test was performed on substance and canopy types using the continuous variables as covariates. An ANOVA test on the coefficient for substance type could not be done because of the high variance inflation factors. Only the data from the trials in Florida were used since the Pennsylvania trials were conducted using only particles. Since the p-values associated with the substance factor were large (much

greater than 0.25), there is no evidence that the spores and particles behave differently under the conditions experienced during the trials in Florida.

Chapter 4

Concentration Profiles and Vertical Escape Flux Estimates

The second objective of this research was to construct concentration profiles of spores and particles and estimate the escape flux (at 1.5 h). The flux of spores Fs (spores m^{-2} s^{-1}) or particles can be estimated from concentration profiles as

Equation **4.1**

$$Fs = -Ks\ (\partial C/\partial z) \qquad \text{Eq. } \mathbf{4.1}$$

where Ks is the diffusivity of spores or particles and $\partial C/\partial z$ is the vertical gradient of spores or particles and can be estimated as $\Delta C/\Delta z$. By assuming the diffusivity of spores or particles is approximately equal to the diffusivity of momentum Km, Ks becomes

Equation **4.2**

$$Ks = Km = u^{*2}/(du/dz) \qquad \text{Eq. } \mathbf{4.2}$$

where u* is the friction velocity (m s^{-1}) and (du/dz) is the rate of change of the average horizontal velocity with height (Aylor et al. 1983). Friction velocity is a reference wind velocity associated with a relationship between the Reynolds stress, the mean forces (per unit area) imposed on the mean wind flow by turbulent fluctuations, and the density of

air. With wind speed measurements at one height, (du/dz) cannot be adequately estimated, however, u* can be estimated from the sonic anemometer measurements as $\sqrt{|w'S'|}$. The measurements w' and S' are the instantaneous deviations from the mean vertical wind speed and horizontal wind speed respectively. Each has units of m s^{-1}.

By assuming that the shape of the wind profile with height is logarithmic above the canopy, wind speed can be estimated by

Equation **4.3**

$$u = (u^*/k)\ln[(z-D)/z_0] \qquad \text{Eq. } \mathbf{4.3}$$

where k is von Karmen's constant (shown experimentally to be equal to 0.4), z is the height (m), D is the displacement height (m) of wind speed, and z_0 is the roughness height (m). Wind speed must equal zero at the surface of the earth, but if the surface contains many roughness elements, the mean horizontal motion equals zero at some height above the surface, the roughness height z_0. Wind flow is changed not only by how tall roughness elements are, but also by how flexible and tightly packed together they are. The displacement height D accounts for this. In an agricultural field, it is often assumed that D = 0.7 h, and z_0 = 0.2 h (Lowry et al. 1989). These values have been used in this analysis.

During the FLCs experiment, spores concentrations measured by rotorod samplers showed a logarithmic relationship with height for each tower. Particle and spore concentrations during all other experiments show a logarithmic relationship with height

on towers downwind of the source during the maximum wind gust. Figure 4.1 shows typical concentration profiles. By assuming spore concentrations C (spores m^{-3}) are logarithmic with height, according to Aylor et al. (1983),

Equation **4.4**

$$C_z = A + B \ln(z-D_s) \qquad \text{Eq. } \mathbf{4.4}$$

where D_s is the displacement height of spore concentrations. The displacement height of spore concentrations may not be exactly equal to D for wind speed, but assuming both are the same usually yields good fits to the data (Aylor et al. 1983). A and B are parameters determined by fitting concentration data for each rotorod tower to Equation 4.4. In the FLCs experiment, data from all towers were used because the source was an area rather than a point. In all other trials, only measurements from the tower that had the greatest spore or particle concentrations were used in the analysis. Towers that were not downwind of the source during the maximum wind gust often did not show a logarithmic relationship with height, and concentrations were also often many orders of magnitude less in value. Only the rotorods at 1.0 h, 1.5 h, and 2.5 h were used in the analysis as the rotorod at 0.5 h was positioned just below the level of D where wind speeds no longer vary with height according to Equation 4.3. After fitting the data to Equation 4.4, the vertical flux of spores and particles was estimated by

Equation **4.5**

$$F = -k\, u^*\, B. \qquad \text{Eq. } \mathbf{4.5}$$

Equation 4.5 takes into account the shape of the profiles of wind speed and concentration by containing the product of the slopes for wind speed and concentration found in Equations 4.3 and 4.4 (Aylor et al. 1983).

Results from the trials can be seen in the data tables in Appendix B. The most data exists for the FLCs experiment trials because the entire field was uniformly infected, and thus data from all four towers could be analyzed. Leaf area index (LAI) did not change much during the 12 FLCs trials, and the data suggest that the vertical flux of spores increased with increasing mechanical turbulence as represented by Max Cov UzS (Fig. 4.2). Spore escape is measured over a 15 minute interval while Max Cov UzS is the maximum 1 minute average of mechanical turbulence during the same interval. The FLCp trials were run simultaneously with the FLCs trials, and the data again suggest vertical fluxes of particles increase with increasing mechanical turbulence (Fig. 4.3). Clearly, the particle flux does not increase as consistently with increasing mechanical turbulence as does the spore flux (Fig. 4.1). This is because the wind direction during the 15 minute trial period varied. Consequently, it is likely that the tower which received the greatest concentration of particles during the 15 minute period was not always downwind of the point source. Conceivably, this tower was not downwind during the 1 minute interval when mechanical turbulence was maximum, the value used in the analysis. Note also that the particle fluxes were greater than those of the spores. This can be attributed to the difference in the type of release. A large number of particles were sifted on to the soybean foliage at one level in the canopy while spores were released naturally from all levels in the canopy. Thus, the particle concentrations at the 0.5 h level close to the release site were far greater than

the spore concentrations at the same level leading to greater source strengths and gradients for particles compared to spores.

During the FLOp and FLOs experiments, the trials were again run simultaneously except for the control trials. Three control trials were conducted during which only particles were released. Subsequent inspection of the rotorod collections indicated that no soybean rust was present in the field throughout the FLO experiment. Again the leaf area index remained nearly unchanged throughout the entire FLO experiment. Vertical spore fluxes out of the canopy increased with increasing mechanical turbulence. During the trials where both particles and spores were released, the fluxes of particles and spores were more similar than the fluxes of particles and spores estimated from the FLCp and FLCs experiments despite the fact that 20 times as many particles were released than spores in the FLO experiment (Fig. 4.4). Assuming the diffusivity of spores and particles was equivalent, the gradients of particle and spore concentration were close to the same, and the vertical escape flux was similar between spores and particles.

The PAp experiment was run throughout the growing season, and both the leaf area index and profile of leaf area changed dramatically throughout the growing season (see Figure 3.5). During the season, the lower canopy concentrations at 0.5 h increased from hundreds or thousands of particles m^{-3} during the open canopy trials (trials 1-4) to tens of thousands of particles m^{-3} in the trials with more mature canopies. This seasonal increase was again seen in the 1.0 h rotorod samples where particle concentrations increased from hundreds to thousands of particles m^{-3}, and finally >18,000 particles m^{-3} in trial 16. The

seasonal increase is less noticeable in the data from the 1.5 h downwind rotorod, and almost completely disappears in the data from 2.5 h (Fig. 4.5). Although the values of turbulence affect a change on vertical particle fluxes, during these trials, F is impacted more by changes in the slope parameter B throughout the growing season (Fig. 4.6). Early in the growing season, the canopy profile is more uniform with height, and during the open canopy trials, the greatest LAI was found at the release height, 20.0 cm. By the end of the Pennsylvania experiment, the top of the canopy was closed and leaves had dropped in the lower canopy with virtually no leaf area in the lowest 30.0 cm. During trials 14-16, 83.0% of the leaf area was above the release height of the particles. Lower canopy transport likely increased as the lower canopy became more ventilated later in the season. This had a dramatic influence on concentrations in the lower canopy (more particles remained airborne within the canopy layer), the slope parameter B calculated using equation 4.4, the concentrations measured at 1.0 h, 1.5 h, and 2.5 h, and the vertical flux F.

Figure **4.1**

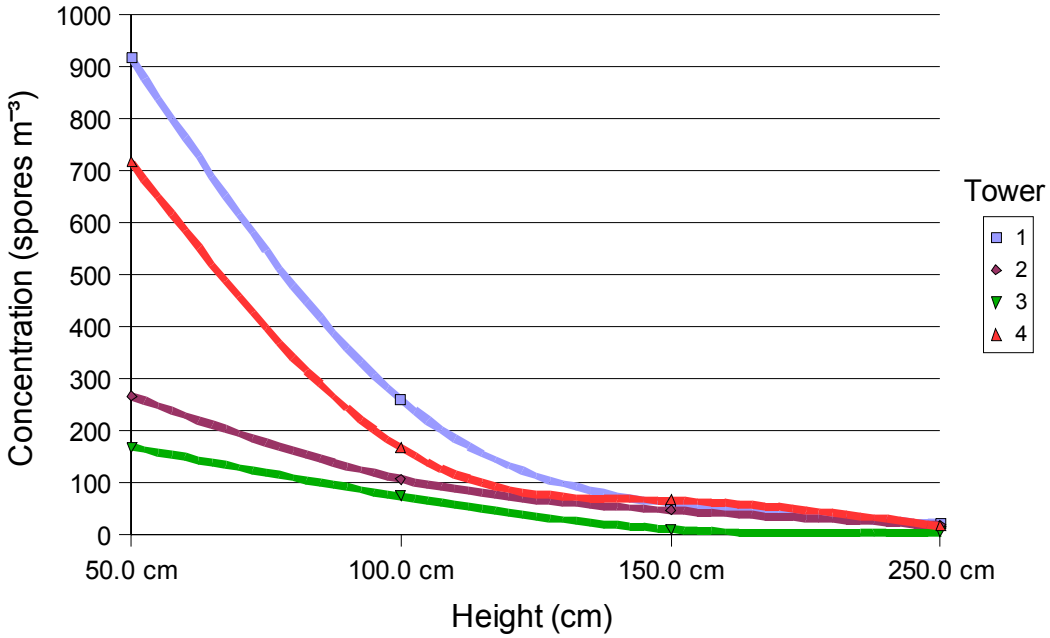

Fig. **4.1**: Spore concentration profiles from trial 11 during the Florida closed canopy spore release experiment. The chart shows a logarithmic relationship with height that is typical for concentration profiles for spores and particles.

Figure **4.2**

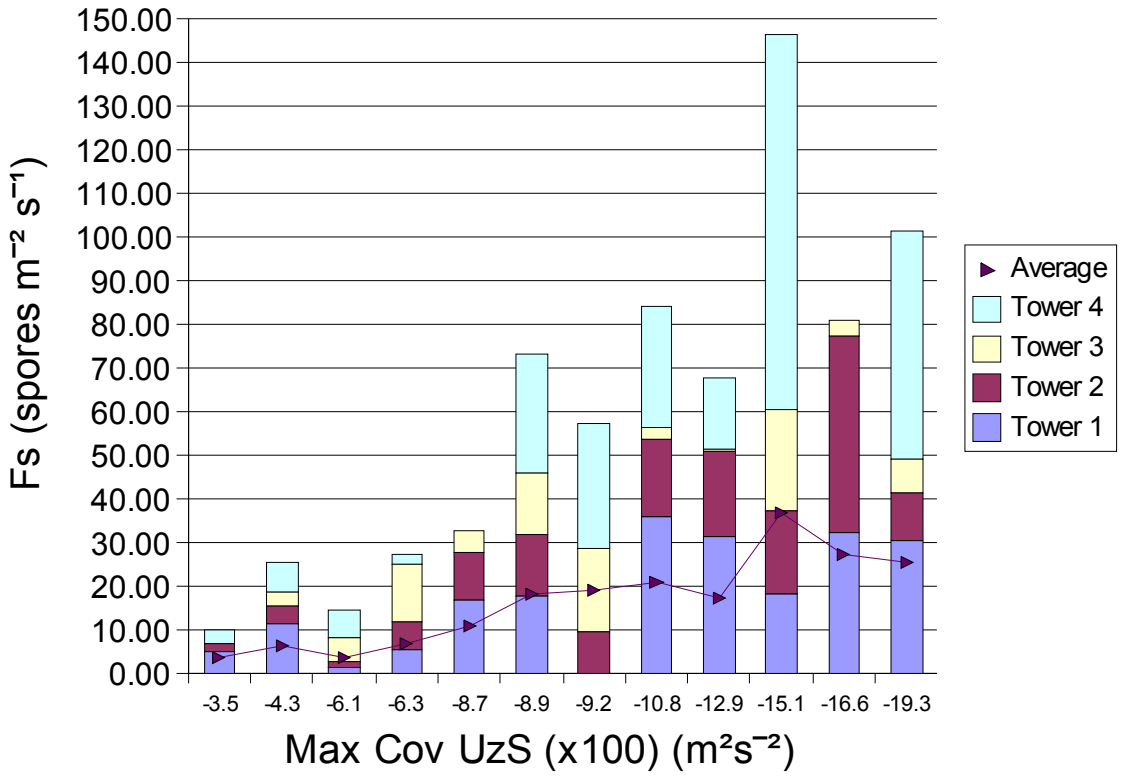

Fig. **4.2**: Vertical fluxes of soybean rust spores out of the canopy (escape) showed an increasing trend with increasing mechanical turbulence (values multiplied by 100). Spore escape is measured over a 15 minute interval while Max Cov UzS is the maximum 1 minute average of mechanical turbulence during the same interval. The line on the chart indicates the average flux for the trials among all four towers.

Figure **4.3**

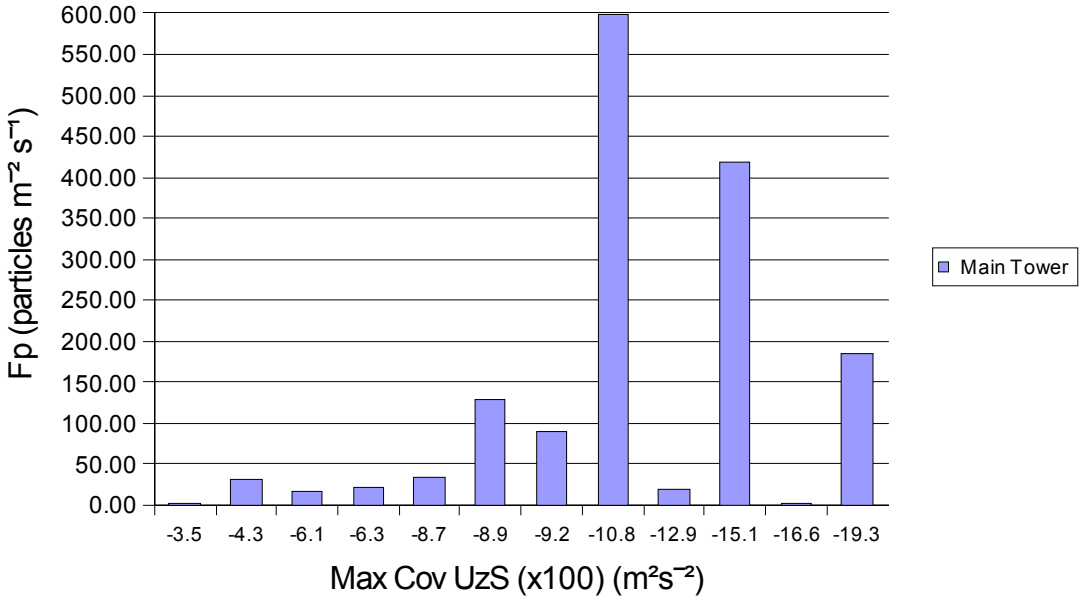

Fig. **4.3**: Vertical fluxes of particles out of the soybean canopy for the FLCp trials showed a trend of increasing values of Fp with increasing mechanical turbulence represented by Max Cov UzS (values multiplied by 100). Particle escape is measured over a 15 minute interval while Max Cov UzS is the maximum 1 minute average of mechanical turbulence during the same interval. However, this relationship is not as obvious as that found in the FLCs experiment. The main tower is the tower whose concentration profile was the highest.

Figure **4.4**

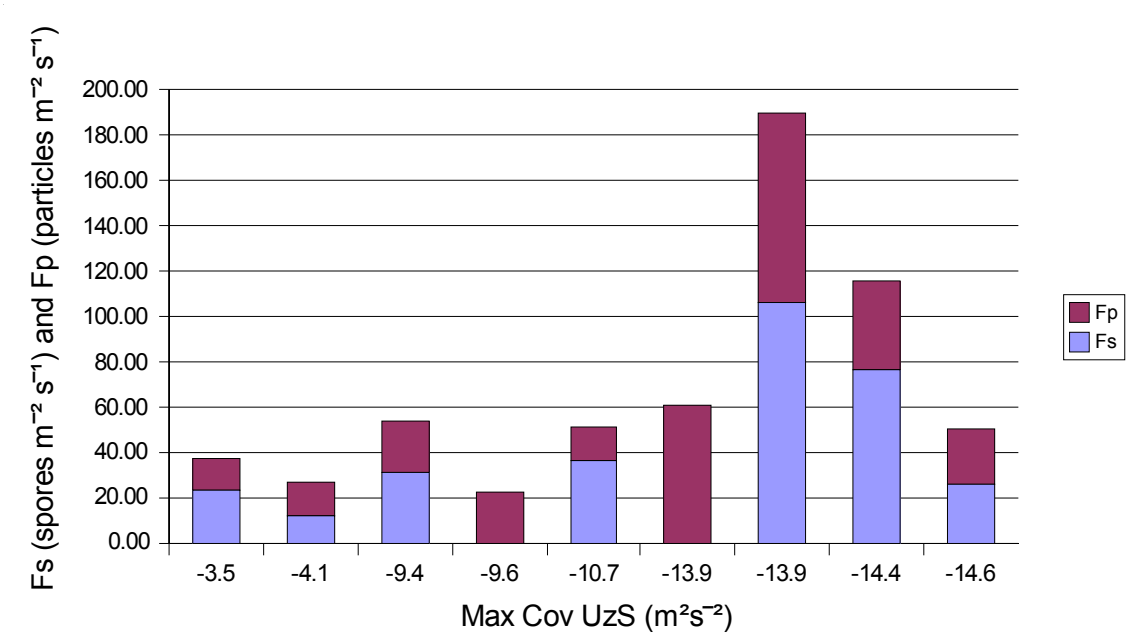

Fig. **4.4**: Particle and spore vertical fluxes (escape) for the FLOp and FLOs trials, respectively, showed a trend of increasing values of Fp and Fs with increasing mechanical turbulence represented by Max Cov UzS (values multiplied by 100). Spore (or particle) escape is measured over a 15 minute interval while Max Cov UzS is the maximum 1 minute average of mechanical turbulence during the same interval. Trials that do not have a value of Fs reported were the controls. Note the similarity in value between Fp and Fs in the open canopy experiments as compared to the closed canopy experiments despite the fact that 20 times more particles were released than spores in the center of the collection grid.

Figure **4.5**

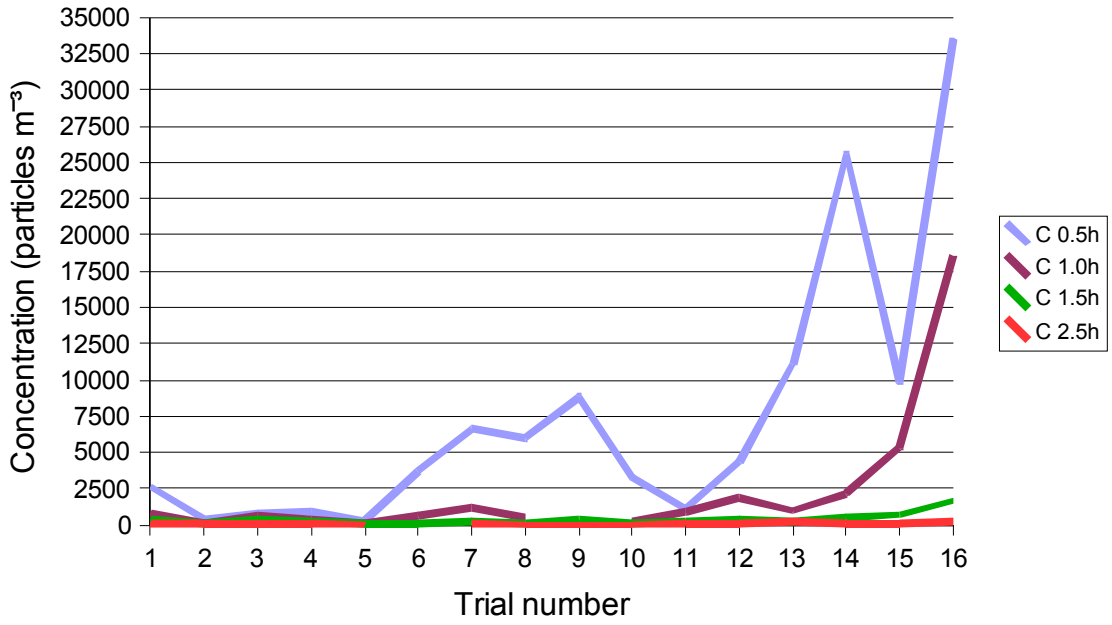

Fig. **4.5**: Particle concentrations at various rotorod heights for each trial during the PAp experiment. Concentration estimates were measured from main towers only. Note the increase in concentration at the two lowest rotorod heights (0.5h and 1.0h) as the season progressed.

Figure **4.6**

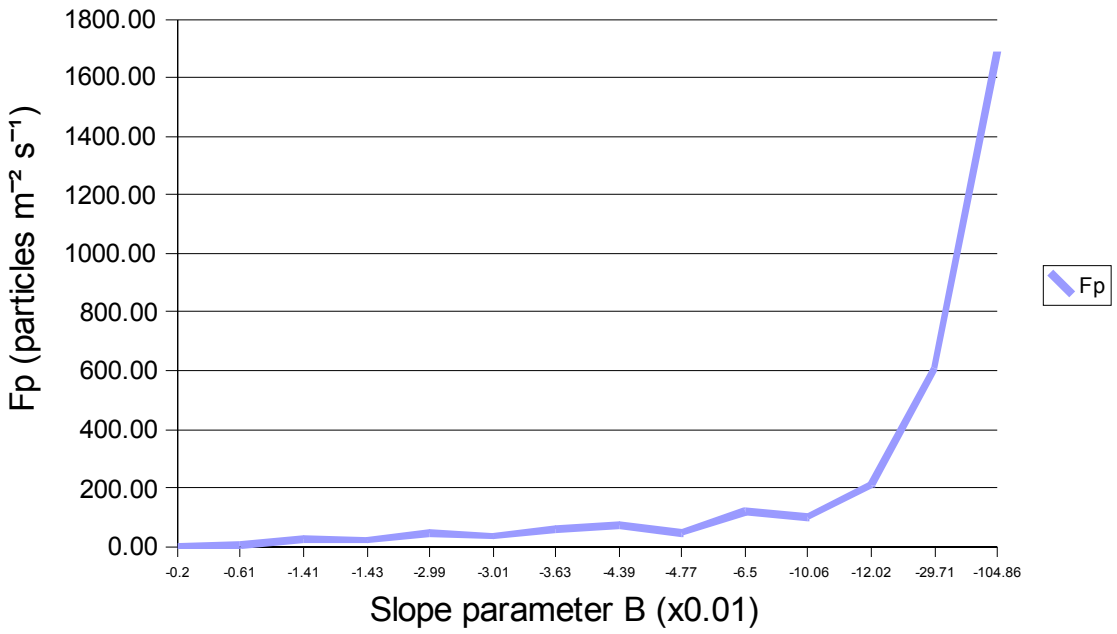

Fig. **4.6**: Vertical fluxes of particles out of the soybean canopy (escape) for the PAp experiment showed a trend toward increasing Fp with increasing values of the slope parameter B from Equation 4.5. B is an indicator of source strength, and an increasing value of B corresponds to an increase in the source strength of particles within the canopy.

Chapter 5

Directional Movement and Vertical Distribution of Spores and Particles

The final objective of this research was to provide a descriptive assessment of the directional and spatial components of movement for spores and particles in and above the canopy. The average horizontal wind velocity was calculated as the 15-minute average of the velocity vectors in the downwind and crosswind directions (u and v respectively) and

were used to calculate the prevailing wind direction. S' and w' are the instantaneous deviations from the mean values of horizontal wind speed and vertical wind velocity respectively. The maximum gust was assumed to have occurred during the period when the one minute average of the covariance of w' and S' (cov w'S') was at its maximum; hereafter, the phrase maximum wind gust is used to indicate the one minute average value for this interval. The average values of u and v during the maximum wind gust interval were used to determine the direction of the maximum wind gust. On occasion, the value of cov w'S' measured at one minute intervals throughout the experiment was not maximum during the same one minute interval when the one minute average wind speed (S_1) was maximum. However, usually the two maxima occurred during the same minute in a 15 minute trial.

5.1 Closed Canopy Florida Experiment (FLC)

During the FLCp and FLCs experiments, winds were lighter and less gusty than during any of the other experiments. Average wind speeds (S_{15}) during the 12 trials ranged from 0.81 to 2.02 m s^{-1} (the subscripts 1 and 15 refer to average wind speeds S calculated at 1 and 15 minute intervals respectively). For the FLCp experiment, the direction of the maximum wind gust was the same as the prevailing wind in 11 of 12 trials. In all of these trials, the lowermost rotorod (0.5 h) on the tower in the collection grid that was downwind for the maximum gust and prevailing wind sampled either: 1) a

volume of air that contained the greatest particle concentration or 2) a volume of air with concentration of the same order of magnitude as the rotorod that had the highest particle concentration. Trial 10 in the FLCp experiment was the only trial in which the direction of the maximum wind gust was not the same as the prevailing wind direction for the entire trial. Tower 1 was downwind of the prevailing wind and its vertical profile had the highest particle concentration. The maximum gust was directed at tower 2, but this tower's profile did not have as great a particle concentration. The value of the cov w'S' for the maximum gust interval was -0.1080 $m^2 s^{-2}$, but the average u and v velocity vectors were less than 1.0 m s^{-1} (u = 0.66 m s^{-1}, v = -0.46 m s^{-1}). Numerous other wind gusts (S1) with values of cov w'S' very close to -0.1080 $m^2 s^{-2}$, including one wind gust with a cov w'S' value of -0.1010 $m^2 s^{-2}$, were directed at tower 1. Although this latter wind gust did not have the greatest value of cov w'S' recorded during the trial, the horizontal velocity vectors were much larger in magnitude (u = 2.55 m s^{-1}, v = 0.64 m s^{-1}) than those associated with the maximum gust interval.

5.2 Open Canopy Florida Experiment (FLO)

Average wind speeds (S15) during the FLO experiment ranged from 0.86 to 2.1 m s^{-1}. Nine trials were conducted during the FLOp experiment, and the direction of the maximum gust was the same as that of the prevailing wind in 7 of the 9 trials. In trial 1, the maximum gust was directed at tower 1, and the profile of particle concentration at the

tower was the highest. The prevailing wind, however, was directed at tower 4. The profile of concentration at tower 4 was of the same order of magnitude as tower 1, but the concentration at each height was roughly 50% that of the profile at tower 1 despite the wind being directed at tower 4 for 10 of the 15 minutes of the trial. During the other 5 minutes of the trial, the winds (S_1), including the maximum wind gust, were directed at tower 1. The maximum wind gust at tower 1 was 2.16 m s^{-1}. No wind speed (S_1) greater than 1.77 m s^{-1} was directed at tower 4, and the average wind speed (S_{15}) directed at tower 4 was 1.42 m s^{-1}.

Trial 6 was conducted at 1000 local time (LT), and wind speeds (S_1) were very light (0.76 – 1.81 m s^{-1}). The cov w'S' only reached a maximum value of -0.0410 m^2 s^{-2} very late in the trial. The wind was directed at tower 4 during this gust, but the prevailing wind along with several other previous wind gusts (S_1) close in magnitude were directed at tower 1 early in the trial. The profile of particle concentration was highest at tower 1.

During the FLOs experiment, the direction of the prevailing wind was the same as the direction of the maximum wind gust in 6 of the 7 trials. During trial 6, most of the spores were collected by rotorods on tower 1 (similar to trial 6 in the FLOp experiment that was conducted simultaneously), which was in the downwind direction of the prevailing wind. Tower 4 was in the downwind direction of the maximum gust. Towers 2, 3, and 4 during this trial had similar profiles of spore concentration. Winds were directed toward tower 1 during the first 5 minutes of the trial when the greatest amount of sifted spores were still on the soybean foliage within the collection grid. The maximum

gust was directed at tower 4 during the 13th minute of the trial, but the cov w'S' was only -0.0410 $m^2 s^{-2}$. During the first 5 minutes of the trial, three gusts (S_1) with cov w'S' values of -0.0350 $m^2 s^{-2}$, -0.0340 $m^2 s^{-2}$, and -0.0330 $m^2 s^{-2}$ were directed at tower 1.

5.3 Pennsylvania Experiment (PAp)

During the PAp experiment, average wind speeds (S_{15}) for the trials ranged from 0.79 to 2.61 m s^{-1}. The PAp experiment had more occurrences of strong wind gusts (S_1) than the Florida trials. The PAp trials were the only ones in which the cov w'S' was greater than -0.20 $m^2 s^{-2}$ (-0.2620 $m^2 s^{-2}$ in trial 15 was the largest representation of the maximum wind gust). The majority of the lowest values of cov w'S' occurred during the FLO and FLC experiments.

The direction of the maximum wind gust was in the same direction as the prevailing wind in 10 of the 16 PAp trials. The particle concentration profiles were highest at the tower(s) that was(were) located downwind of the maximum wind gust in 11 of the 16 trials and downwind of the prevailing wind in 9 of the 16 trials. Of the six trials where the direction of the prevailing wind differed from that of the maximum wind gust, in two of the trials the tower downwind of the maximum wind gust had the highest concentrations in its profile. In three of these trials, towers located downwind of the prevailing wind and maximum gust had particle concentration profiles of equal order of

magnitude. In trial 4, the concentration profile at tower 1 was the highest, and the concentration profile at tower 4 was of an equal order of magnitude (although the particle concentration profile at tower 4 contained less than 50% of the particles in the profile at tower 1). The maximum wind gust was directed at tower 1 during the first minute of the experiment, while the wind was directed at tower 4 for the remainder of the trial. Trial 15 was similar to trial 4, however, the maximum wind gust was directed at tower 1 in the 4^{th} minute of the trial. Tower 4 was again downwind of the prevailing wind, and had a concentration profile the same order of magnitude of particles as the profile at tower 1. The particle concentration profile at tower 4 contained about 25% of the particles in the profile at tower 1. The maximum value of cov w'S' observed during the entire research project occurred during this trial and was directed at tower 1. Finally, in trial 11, neither the prevailing wind nor the maximum wind gust recorded was in the direction of the tower with the greatest particle concentration profile. The wind direction was quite variable during this trial, and it is conceivable that relatively strong, short wind gusts lasting only a few seconds could have occurred whose directions were not recorded by the one minute average of cov w'S'.

5.4 Transport within Aging and Diseased Canopies

During the PAp experiment, the greatest number of particles caught inside the canopy at the 0.5 h and 1.0 h rotorod heights occurred in the final 4 trials. The PAp

experiment was conducted throughout the growing season, and by the final trials many of the leaves in the lower canopy had dropped (see Figure 3.5). In the FLOp trials, concentrations of particles in the lower canopy were less than the concentrations found in the lower canopy in the FLCp trials. Figures 5.1 and 5.2 show the leaf area profile at the start and finish of the FLCp experiment. Not only was the canopy in the FLCp experiment at an advanced stage of development, it was also severely diseased. This likely aided in lower canopy transport as well as the proportion of particles escaping the canopy. While the proportion of escaping spores was greater in an open canopy than a closed canopy, transport within the canopy was hindered in open and younger canopies by an increase in the proportion of leaf area in the lower portions of the canopy. The diseased canopy in the FLC experiment became more ventilated as the leaves died and the canopy matured. The canopy in the PAp experiment became more ventilated as the canopy matured.

5.5 Crosswind and Upwind Transport

In general, during trials in which spores and/or particles were released from a point source in the center of the collection grid, the concentration profiles at towers that were not downwind of the prevailing wind or the maximum wind gust contained concentrations of particles or spores that were at least an order of magnitude (and often times many orders of magnitude) less than the spore or particle profile of concentration

on towers that were downwind of prevailing winds and maximum wind gusts. In many of the trials conducted in open canopies, the towers that were not downwind of the prevailing wind or maximum wind gust show profiles of concentration that increased with height, particularly between the 1.0 h and 1.5 h rotorod. Figures 5.3 and 5.4 show this relationship in open and closed soybean canopies.

Figure **5.1**

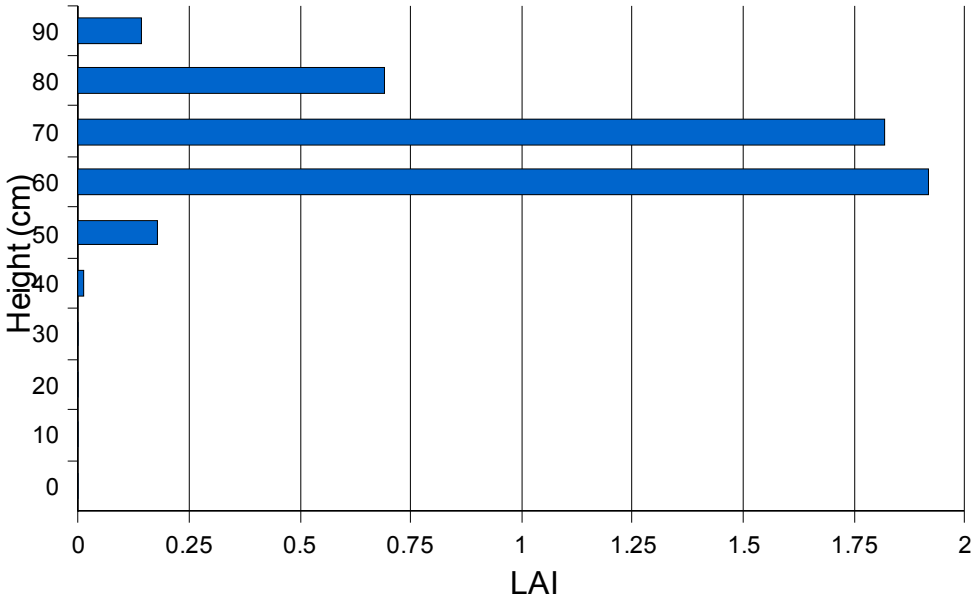

Fig. **5.1**: Leaf area index (LAI) measurements at 10.0 cm height intervals within the closed soybean canopy in Florida (FLC) taken on 23 August 2006. Canopy height was 100.0 cm. Total LAI was 4.77. LAI above 0.5 h was 4.76. Particles were released at 0.5 h (50.0 cm).

Figure **5.2**

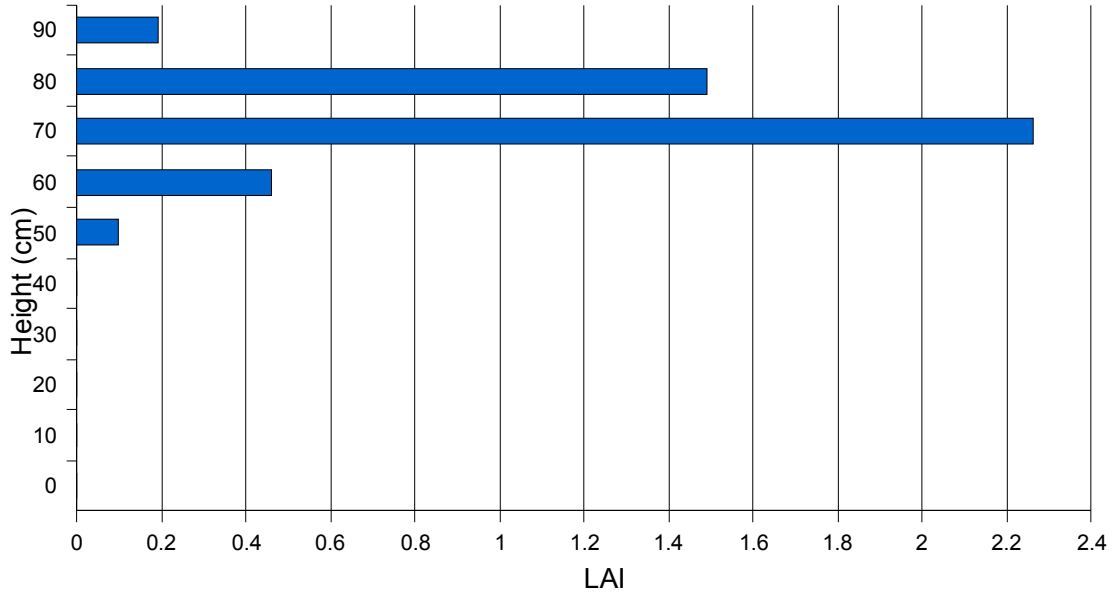

Fig. **5.2**: Leaf area index (LAI) measurements at 10.0 cm height intervals within the closed soybean canopy in Florida (FLC) taken on 28 August 2006. Canopy height was 100.0 cm. Total LAI was 4.49. LAI above 0.5 h was 4.49. Particles were released at 0.5 h (50.0 cm).

Figure **5.3**

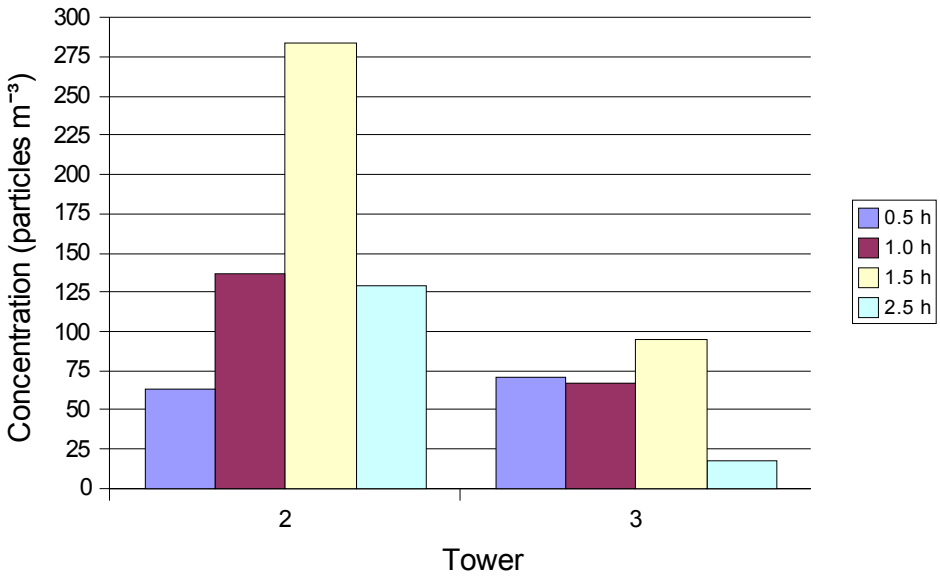

Fig. **5.3**: Particle concentrations from towers that were not downwind of the maximum wind gust or the prevailing wind taken in an open soybean canopy in Pennsylvania. Towers 1 and 4 were located in the direction of the maximum gust and prevailing wind for the trial respectively. Note the increase in particle concentration with height below 2.5 h.

Figure **5.4**

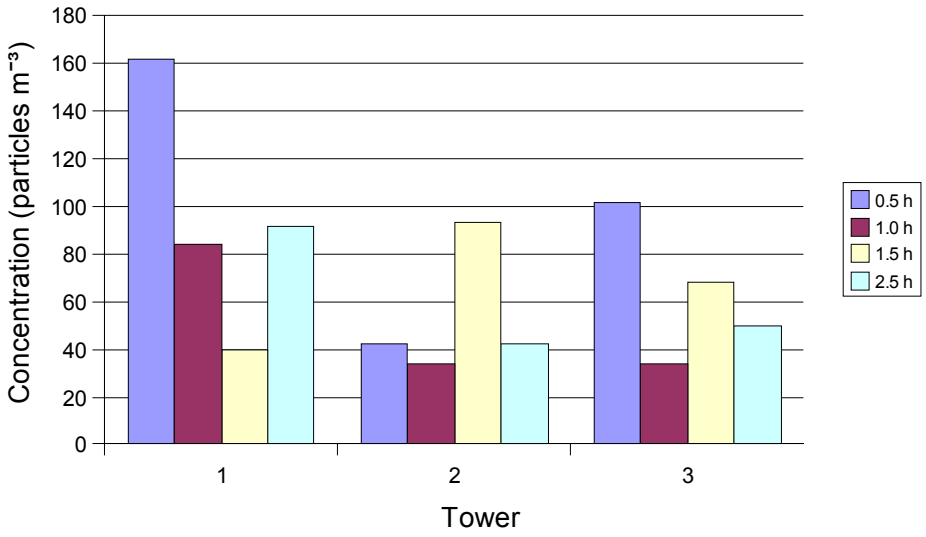

Fig. **5.4**: Particle concentrations from towers that were not downwind of the maximum wind gust or prevailing wind taken in a closed soybean canopy in Florida. Tower 4 was located downwind of the maximum wind gust and the prevailing wind.

Figures 5.5 and 5.6 show the relative shape of particle or spore clouds during two separate types of wind conditions: strong and gusty (Fig. 5.5) and light and variable (Fig. 5.6). Figure 5.5 shows the relative particle cloud shape at each rotorod height during a closed canopy trial in Pennsylvania. During this trial, winds (S1) were directed at both tower 2 and tower 3, but the maximum gust, as well as the majority of the particles, were directed toward tower 3. Figure 5.6 shows the relative spore cloud shape at each rotorod height during an open canopy trial in Florida in which the winds were lighter and more variable. The maximum gust and prevailing wind were both directed toward tower 4, but winds (S1) were also directed at towers 1 and 3 during the trial. Relative to the particle clouds shown in Figure 5.5, it seems that the a greater proportion of the spores in the

spore cloud in Figure 5.6 spread more in the crosswind and upwind directions compared to the downwind direction at each rotorod height. At the highest rotorods (1.5 h and 2.5 h), a near equal distribution of spores were caught by rotorods at each of the four towers.

Figure **5.5**

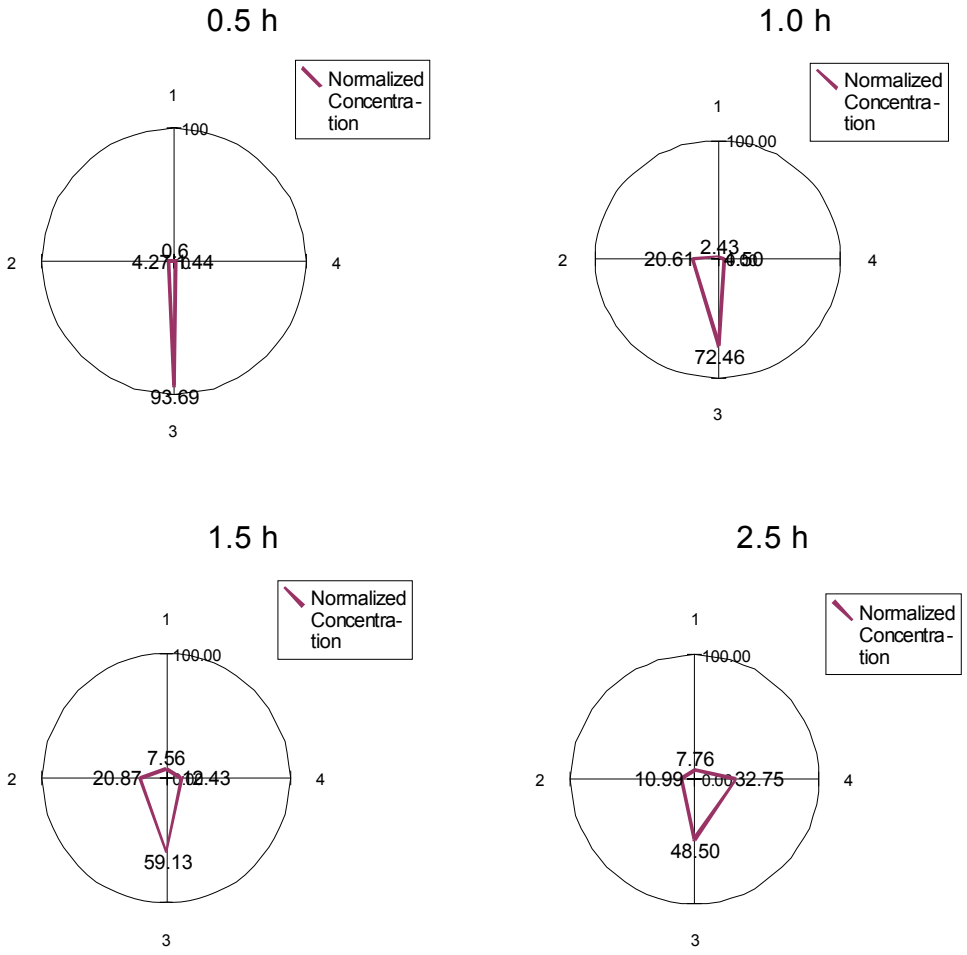

Fig. **5.5**: Normalized concentration (concentration of particles at rotorod height divided by the sum total concentration at all rotorod heights on the same tower) at each rotorod height on all four towers during the Pennsylvania particle escape experiment (PAp) trial 13. The prevailing winds were directed at tower 2, and the maximum wind gust (cov w'S' = -0.1610 m^2s^2) was directed at tower 3. Note the change in the shape of the particle cloud with height. The relatively strong wind gust directed the most particles toward tower 3 at each height, but the relative percent of the total concentration decreases with height. The canopy was closed during this trial, and the lower canopy was more ventilated than the previous trials conducted immediately after canopy closure.

Figure **5.6**

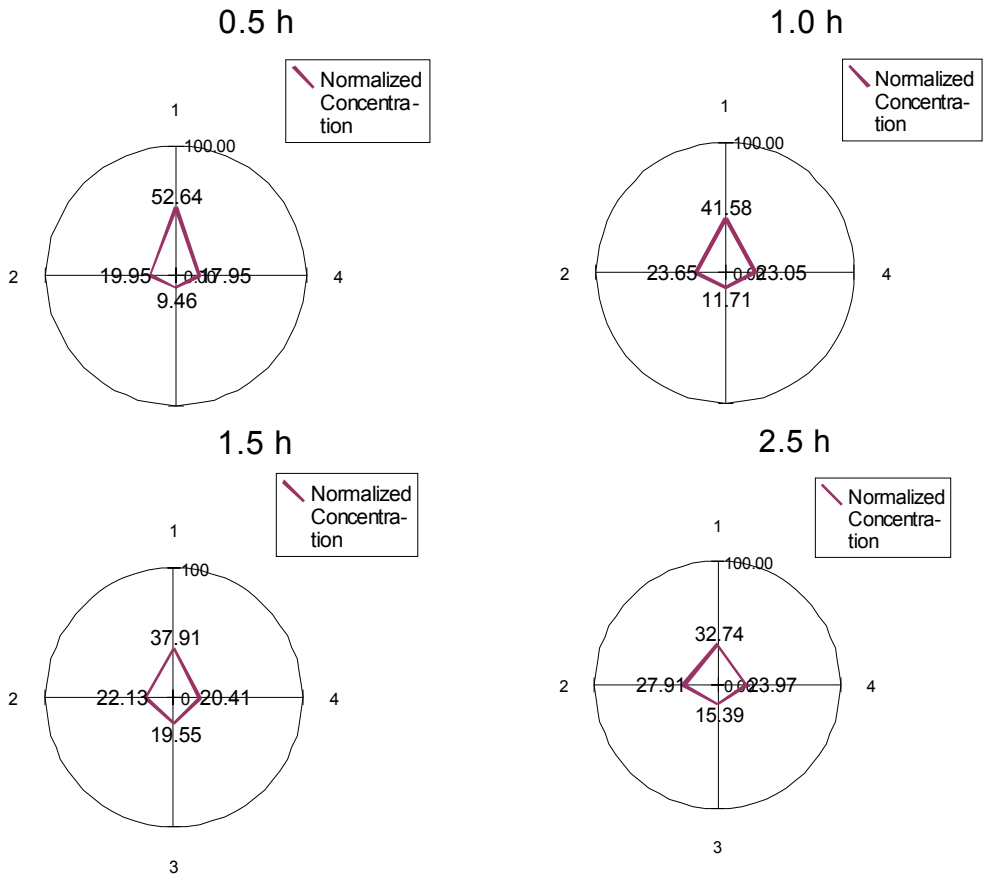

Fig. **5.6**: Normalized concentration (concentration of particles at rotorod height divided by the sum total concentration at all rotorod heights on the same tower) at each rotorod height on all four towers during the Florida open canopy spore escape experiment (FLOs) trial 4. The prevailing winds and maximum gust (cov w'S' = -0.1070 m^2s^2) were directed at tower 4, but winds (S_1) were also directed at towers 1 and 3. Note the change in the shape of the particle cloud with height. A greater proportion of spores were caught on towers located in the crosswind and upwind directions relative to the downwind direction than was observed when wind speeds (S_1) were greater.

Chapter 6

Discussion

6.1 Spore/Particle Escape

The first objective of this research was to estimate the proportion of released spores that escape from a soybean canopy and relate that value to environmental variables such as mechanical turbulence and also to attributes of canopy structure such as leaf area index (LAI). No statistical difference was found between the behavior of spores and particles under the conditions experienced during the research project.

6.2 Canopy Types – Open, Closed, Healthy, and Diseased

The first notable difference in escape proportions is between open and closed canopies. An open canopy was more ventilated and allowed more released spores or particles to escape. On average, roughly 26% of spores or particles escaped from open soybean canopies, while only about 10% of spores or particles escaped from closed canopies (Tab. 6.1).

Table **6.1**

Tab. **6.1**: Summary of spore or particle escape proportion (%) for each experiment, canopy type (open and closed), and substance. The escape proportion was estimated as the proportion of spore or particle concentration at 1.5 h to the concentration at 0.5 h on the same tower.

Experiment	Substance	Canopy	Escape % (1.5h)
Pennsylvania	particles	open	24.0
Florida	particles	open	25.7
Florida	spores	open	30.4
Pennsylvania	particles	closed	6.3
Florida	particles	closed	14.1
Florida	spores	closed	12.2

The proportion of spores or particles escaping a canopy was reduced once the canopy closed. The lowest escape percentage (6.3%) was observed in the Pennsylvania closed canopy trials using particles. It is likely that the escape proportion was reduced relative to the Florida closed canopy trials for both particles and spores because of the reduction in leaf area in the canopy in Florida due to the severity of the disease. It appears from the data that a severely diseased canopy similar in age to a healthy canopy allowed for a greater proportion of released spores and particles to escape. The last total LAI measurements taken in the soybean canopies in Pennsylvania and Florida were 6.09 and 4.49 respectively.

6.3 Escape Regression Models

The experiments were modeled separately by substance, then by canopy, and finally all trials combined. Table 6.2 summarizes the results from the models as well as important

predictor variables. When modeled separately by canopy type and substance, LAI was an important predictor in models during experiment period where LAI varied. When canopy types were combined, LAI was not an important predictor variable. Whether the soybean canopy was open or closed, and how mechanical turbulence interacted with the different types of canopy structures were the best predictor variables.

Relating to the first objective, mechanical turbulence and canopy structure, whether expressed as LAI above the release height or as a categorical variable ('open' or 'closed'), proved to be important predictor variables in estimating the proportion of released spores or particles that escape a soybean canopy. Other important predictors were the height of the rotorod at 1.5 h, the Monin-Obukhov stability parameter (see Appendix A), and the following interactions: LAI and stability, LAI and mechanical turbulence, and canopy structure and mechanical turbulence.

Table **6.2**

Tab. **6.2**: Regression model fits and important predictor variables for the various experiments modeled separately and combined (H is the height of the rotorod in cm, T is the mechanical turbulence expressed as the maximum covariance of w' and S', s is the Monin-Obukhov stability parameter, LAI is the leaf area index, substance is a categorical indicator for the type of substance, and canopy is a categorical indicator for an open or closed canopy). No satisfactory relationship was found for the closed canopy particle trials in either Florida or Pennsylvania. The closed canopy spore trials were conducted in a severely diseased soybean field, and the spores were released naturally under ambient environmental conditions. In all other trials, either spores or particles were sifted onto the soybean foliage immediately prior to sampling.

Experiment	R-sq (%)	p	Predictor variables
Open canopy spores	90.6	< 0.05	H T s
Closed canopy spores	77.8	0.055	T LAI s LAI*s LAI*T
Open canopy particles	79.4	< 0.05	H T LAI
Open canopy combined	81.8	< 0.05	H T LAI substance
All types (no closed canopy particles)	67.2	< 0.05	LAI s LAI*s
Entire project period	48.6	< 0.05	T canopy T*canopy

6.4 Estimated Spore and Particle Escape Flux from Concentration Profiles

The second objective of this research was to construct concentration profiles of spores and particles and estimate the escape flux. The spore and particle escape flux was estimated using assumptions of a logarithmic concentration profile and a logarithmic wind profile (Aylor et al. 1983). Although the concentration profile appeared to be logarithmic (see Figure 4.1), the lowest rotorod (0.5 h) was not included in the estimation of escape flux because it was located below the zero-plane displacement height (0.7 h for soybeans), and thus below the height at which the wind profile was assumed to be logarithmic.

6.5 Escape Flux in Closed Canopy Florida Trials (FLCs and FLCp)

During the FLCs experiment, the LAI did not change significantly, and the estimate of the vertical escape flux depended mainly on the wind profile rather than the strength of the source. The flux of spores escaping showed an increase with increasing mechanical turbulence. This was the only experiment in which spores were released naturally under ambient environmental conditions in a severely diseased soybean field. The vertical escape flux of particles during the FLCp trials also showed an increase in the vertical escape flux with increasing mechanical turbulence, however, the relationship was not as obvious as that found in the FLCs experiment.

6.6 Escape Flux Estimates in Open Canopy Florida Experiments (FLOs and FLOp)

The FLOp and FLOs experiments were run simultaneously, and the vertical escape flux of spores and particles both showed an increasing trend with increasing values of mechanical turbulence. Assuming that the diffusivity of spores was the same as the diffusivity of particles, the gradients of particle and spore concentration were close to the same, and the vertical escape flux was similar between spores and particles despite 20 times more particles released per trial than spores.

6.7 Escape Flux Estimates in the Pennsylvania Experiment (PAp)

The PAp experiment was conducted over an entire growing season, and the vertical escape flux increased as the season progressed. In the beginning of the season, a greater proportion of the total LAI was located in the lower half of the canopy, but by the end of the season, most of the total LAI was located in the top 20-30 cm of the canopy. Because of this, the lower canopy became more ventilated late in the season allowing for more lower canopy transport. The concentration of particles in the lower part of the canopy became so great during the final 3 trials that the source strength rather than the mechanical turbulence became the dominant factor for estimating vertical escape fluxes.

6.8 Directional and Spatial Components

The third objective of this research was to provide a qualitative description of the directional and spatial components of spore and particle transport within and just above the canopy for all the experiments in which spores or particles were released as a point source in the center of the collection grid. The most important point of note was the apparent response to wind gusts as opposed to prevailing winds for the movement of

spores. In most cases, a tower in the direction of the maximum gust had a profile with concentrations of the greatest order of magnitude. This was especially true when the maximum wind gust occurred early (within the first few minutes) of a trial. If the gust occurred later in the trial, and particularly if the gust was in a different direction than the prevailing wind direction, the tower in the direction of the prevailing wind typically had profiles of the same order of magnitude, if not greater, than the tower in the direction of the maximum gust.

The strength of the wind gust also appeared to be important in the transport of the spores or particles in and just above the canopy. Figures 5.5 and 5.6 show the difference in the shape of the cloud of spores or particles being transported. The maximum gust was directed at a different tower from the prevailing wind (see Fig. 5.5), but the gust was strong and directed the majority of the particles toward tower 3 (the tower in the direction of the maximum gust during the trial). However, with increasing height from the 0.5 h rotorod to the 2.5 h rotorod, the concentrations at the crosswind and upwind towers increased relative to the downwind direction indicating an increase in turbulent transport with height. This was true for most of the trials in which the winds were stronger and more turbulent (more wind gusts). When the winds were lighter and more variable (see Fig. 5.6), the concentrations in the crosswind and upwind directions were nearly as high as the concentration in the downwind direction.

6.9 Ventilated Canopies

As the season progressed, the soybean plants senesced their lowermost leaves, and the canopy became open. Looking at the Florida closed canopy particle experiment (FLCp) and the closed canopy trials from the Pennsylvania particle experiment (PAp), the concentrations at the 0.5 h rotorods were much greater than in any other trials. The FLCs experiment could not be evaluated for lower canopy transport because the spores were released at varying heights throughout the canopy in densities relative to LAI at that particular height. During most of the season, currents of air hit the edge of the field and were pushed upward, similar to winds being pushed over a building or a mountain (Rosenberg et al., 1983). However, late in the season the current of air was most likely split with some of the forward moving air being push above the canopy and over the foliage and some moving straight through the canopy below the foliage and in between the stems. This type of airflow could be the reason why no satisfactory relationship could be found describing escape of particles released from a point source for any of the closed canopy particle trials (FLCp and closed canopy PAp).

6.10 Spore/Particle Clumping

Spore and particle clumping were recorded from singlets to quadruplets. Any clump with five or more spores or particles was recorded in one category labeled ‘5+’. Tables 6.3 and 6.4 show the number of singlets relative to that of doublets, triplets, quadruplets, and

clumps with 5 or more spores or particles for open and closed canopy spore trials as well as open and closed canopy particle trials. The data for escape of singlets relative to doublets and triplets for both spores and particles and open and closed canopies agrees with Aylor and Ferrandino (1985). Their data showed that the escape rate of singlets of urediniospores of *Uromyces phaseoli* from a typical bean canopy relative to doublets and triplets were 2-7 times greater and 5-30 times greater respectively. No discernable difference in escape rates for clumps existed between open and closed canopies for trials using particles. For trials using spores, the escape rate of clumps of spores was greater in open canopies than closed canopies. However, the difference in release type (point source versus natural release under ambient environmental conditions) diminishes any meaningful comparison between spore clump escape rates for open and closed canopies.

Table **6.3**

Tab. **6.3**: Escape rate of singlets relative to doublets and triplets of spores and particles in open and closed soybean canopies. During the closed canopy spore trials, the spores were released naturally under ambient environmental conditions. During all other trials, the spores or particles were sifted onto the soybean foliage at 0.5 h immediately prior to sampling. The mean indicates how many times more singlets escaped than doublets or triplets. The count is the number of trials.

Closed Canopy Spore Trials

Doublets		*Triplets*	
Mean	10.2	Mean	38.4
Standard Error	2.1	Standard Error	9.0
Count	12	Count	12
Confidence Level(95.0%)	4.5	Confidence Level(95.0%)	19.8

Open Canopy Spore Trials

Doublets		*Triplets*	
Mean	13.6	Mean	89.5
Standard Error	2.1	Standard Error	25.5
Count	7	Count	7
Confidence Level(95.0%)	5.2	Confidence Level(95.0%)	62.4

Open Canopy Particle Trials

Doublets		*Triplets*	
Mean	3.4	Mean	9.5
Standard Error	0.7	Standard Error	1.7
Count	13	Count	12
Confidence Level(95.0%)	1.5	Confidence Level(95.0%)	3.7

Closed Canopy Particle Trials

Doublets		*Triplets*	
Mean	3.3	Mean	12.9
Standard Error	0.4	Standard Error	4.1
Count	24	Count	23
Confidence Level(95.0%)	0.8	Confidence Level(95.0%)	8.5

Table **6.4**

Tab. **6.4**: Escape rate of singlets relative to quadruplets and clumps with 5 or more spores or particles. Results are separated into trials conducted in open and closed soybean canopies. During the closed canopy spore trials, the spores were released naturally under ambient environmental conditions. During all other trials, the spores or particles were sifted onto the soybean foliage at 0.5 h immediately prior to sampling. The mean indicates how many times more singlets escaped than quadruplets of clumps with 5 or more spores or particles. The count is the number of trials.

Closed Canopy Spore Trials			
Quadruplets		*5+*	
Mean	67.6	Mean	63.8
Standard Error	13.2	Standard Error	16.7
Count	10	Count	8
Confidence Level(95.0%)	29.8	Confidence Level(95.0%)	39.5

Open Canopy Spore Trials			
Quadruplets		*5+*	
Mean	382.6	Mean	286.5
Standard Error	139.1	Standard Error	116.3
Count	6	Count	3
Confidence Level(95.0%)	357.6	Confidence Level(95.0%)	500.4

Open Canopy Particle Trials			
Quadruplets		*5+*	
Mean	26.1	Mean	52.8
Standard Error	5.2	Standard Error	17.2
Count	11	Count	8
Confidence Level(95.0%)	11.6	Confidence Level(95.0%)	40.6

Closed Canopy Particle Trials			
Quadruplets		*5+*	
Mean	32.8	Mean	64.3
Standard Error	6.5	Standard Error	10.6
Count	18	Count	16
Confidence Level(95.0%)	13.6	Confidence Level(95.0%)	22.5

6.11 Long Distance Transport Scenario (MS to IL)

Following a transport scenario for tobacco blue mold from Texas to Kentucky in 1985 (see Isard and Gage, 2001; also see Davis and Main, 1990; Aylor and Taylor, 1983; Rotem and Aylor, 1984; and Aylor 1986), a similar scenario can be developed for long distance transport of soybean rust from the gulf coast to the major soybean producing areas of the Midwest. A straight line flight from Mississippi to Illinois is roughly 1600 km. A transport dilution factor τ used in Aylor (1986) for tobacco blue mold can be assumed to be similar to τ for soybeans and computed as

Equation **6.1**

$$\tau = (P\pi Sx^2)^{-1} = 1.73x10\text{^-}14\ m^{-3} \qquad \text{Eq. } \mathbf{6.1}$$

where P is the planetary boundary layer height (2000 m) and S_x is the radius of the spore cloud (m) = 0.5 t where t is the travel time. Assuming 53.3 hours (192000 s) of transport (assuming 850 mb winds of 30 km hr^{-1} for 1600 km), survivorship of spores s = 0.01, and wet deposition velocity v_w = 2.3 m s^{-1}, a deposition flux δ (spores m^{-2} s^{-1}) for soybean rust spores originating in Mississippi that could infect major soybean areas in Illinois can be calculated as

Equation **6.2**

$$\delta = N_0\ \tau\ s\ v_w \qquad \text{Eq. } \mathbf{6.2}$$

where N_0 is original number of viable spores in the Mississippi source region. N_0 depends on factors such as: percentage of the daily total of released spores that are released during the time period applicable for transport and the amount of the spores released that escape a canopy. The same modeling assumptions that are found in Isard et al. (2005) can be used to estimate N_0. The assumptions are as follows: planting density is 500000 plants per ha, 25% of the soybean crop is heavily infected with soybean rust (125000 infected plants) (Isard et al., 2005), and 6 million spores are released each day per infected plant (Melching et al., 1989 and Yang et al. 1990). Thus, the daily total spores released each day from one ha of soybean plants is 7.5×10^{11} spores ha^{-1} or 75 million spores m^{-2}. Considering only spores released during the late morning and very early afternoon (roughly 1/3 of the daily total) and assuming spore escape rates of 0.30 and 0.12 for open and closed canopies respectively (see Table 6.1), N_0 is equal to 7.42 million and 2.97 million spores m^{-2} for open and closed canopies respectively. Thus, Equation 6.2 gives an estimate for δ of 2.95x10^-9 spores $m^{-2}s^{-1}$ for open canopies and 1.18x10^-9 spores $m^{-2}s^{-1}$ for closed canopies. Using S_x for the spore cloud length in the downwind direction and again assuming an 850 mb level average wind speed for the entire 53.3 hours transport of 30 km hr^{-1}, the amount of time required for the spore cloud to pass over a destination soybean field in Illinois is roughly (96000 m / 8.33 m s^{-1}) 11524 s. Integrating the spore deposition rate over the amount of time required to pass over the fields

Equation **6.3**

$$\delta(T) = \int \delta \, dt, \; t = 0 \rightarrow 11524 \text{ s} \qquad \text{Eq. } \mathbf{6.3}$$

gives the total amount of spores deposited per unit area over the entire time period that the spore cloud was above the destination field. Using estimated from Equations 6.1 and 6.2, the total seed deposition flux is roughly 3.4x10^-5 spores $m^{-2}s^{-1}$ for open canopies and 1.4x10^-5 spores $m^{-2}s^{-1}$ for closed canopies. Converting to the units used in the transport model in Isard et al. (2005), the seed depositions are roughly 29,000 spores ha^{-1} day^{-1} for an open canopy and 12,000 spores ha^{-1} day^{-1} for a closed canopy. The spread of soybean rust into the Lower Ohio River Valley during September-October 2006 from source areas in Louisiana and Mississippi was an example of long distance spread of soybean rust over several thousand km. In portions of western Kentucky, the deposition of spores was roughly 1000 spores ha^{-1} day^{-1} (Isard et al., in press).

6.12 Seasonal Soybean Rust Development Scenario

During the early part of the season, the soybeans are in the vegetative stage and are not as susceptible to soybean rust. As the early season progresses and flowering is reached, the disease can begin to form in the lower canopy if the canopy microclimate conditions are suitable (see Section 1.2). The disease likely shows symptoms in the lower canopy first because this location is where temperature, moisture, and radiation conditions are more conducive for disease development. During the earliest of reproductive stages, the leaf area is more uniform with height with a greater proportion of the total leaf area in the

lowest half of the canopy compared to the late season. At this point, the zone in the soybean canopy most conducive for disease development is widest, there is less total leaf area between the originating spore source and the open air above the canopy for the spores to escape, and the canopy may or may not be closed. If the canopy is closed, the microclimate may be more suitable for survivability of the spores within the canopy, however the proportion of released spores that escape is reduced. Alternatively, if the canopy is still open, stronger wind speeds will be able to penetrate deeper into the canopy layer and a greater proportion of released spores will escape the canopy. However, the microclimate is not as suitable for survivability of spores due to increased penetration of solar radiation killing the spores directly or indirectly by heating the soil surface and consequently the air just above the surface more than in the closed canopy scenario. Thus, the zone within the canopy conducive for disease development is squeezed from below.

By the middle of the growing season, the canopy is typically closed and some of the lowest leaves in the canopy begin to senesce. The leaf area profile has a greater proportion of the total leaf area in the upper layers of the canopy, and the disease also moves upward within the canopy. While the total leaf area is still increasing, the disease source is also moving upward in the canopy which serves to reduce the total number of leaves a vertically traveling spore must miss before escaping the canopy. The solar radiation in the upper part of the canopy limits the suitability for spore survivability in the uppermost parts of the canopy, and the increased airflow in the lower parts of the canopy reduces the time to drying in the lowermost parts of the canopy and limits the suitability

for spore survivability there. During this part of the growing season, the zone conducive for spore production shrinks by being squeezed from above and below.

Later in the season, the canopy strops growing taller, leaves have senesced from the lowest parts of the canopy, and the vast majority of the total leaf area is in the top 20-30 cm of the canopy. The major production of spores still moves further upward within the canopy as the zone suitable for production moves upward in accordance with the leaf area. However, the zone is still limited from above by solar radiation, and is now limited from below by even more ventilation and by the senescence of the soybean plant itself. During this part of the growing season, the canopy is so ventilated that the wind flow approaching a soybean field is likely split with some of the forward moving air pushed upward over the canopy and some forced downward and underneath the canopy along the surface. With a secondary maxima of wind speed within the canopy above the surface and underneath leaves, turbulent eddies can force released spores from above to move downward with more frequency. Since there are no leaves between the released spores and the ground, these spores will either fall to the ground and perish or be transported within the canopy to be moved either upward to collide with other leaves above or to the edge of the field and beyond on air currents.

It has been shown that the proportion of released spores that escape a canopy depend, at least in part, on the canopy structure. Whether the canopy is open or closed was shown to be an important attribute in the spore escape process. However, the total number of spores released may be the greatest risk factor for long-distance transport. Typically,

fields with open canopies early in the season may have a few spots in the field with symptoms of soybean rust, but on the whole, the severity is often quite low. Despite the fact that roughly 25-30% of these released spores will escape the canopy, the total number actually escaping is quite a bit less than a more mature field with a closed canopy, high severity, and only a 10-12% escape rate. While the former scenario still can provide spores capable of long distance transport and disease spread, the latter case is more likely a higher risk as the turbulent air motions of the atmosphere will take more time to dilute the spore cloud such that airborne concentrations reach a minimum value posing a risk for disease spread. For example, suppose 1 spore per m^3 of air is necessary for a meaningful risk of infection 1000 km away from a source field. During the open canopy example above, perhaps the time it takes for a horizontally transported cloud of spores to be diluted such that 1 spore m^{-3} is the concentration of the spore cloud occurs in the first 100 m to maybe 1 km of horizontal transport in the atmosphere. During the latter case, perhaps this limiting concentration of the spore cloud will be reached at a much later time during transport, many hundreds to thousands of km away from the source field. This could be a reason why long distance movement has not occurred in the United States until later in the growing season. Presumably, the disease could overwinter during a warm winter in such quantities as to initiate more severe disease outbreaks earlier in the season. If these initial outbreaks are followed by conditions conducive for local disease development and spread, the timing of the long distance spread northward from the southern United States could shift earlier in the growing season to the point where it would be quite damaging economically in the major growing soybean areas of the northern half of the United States.

Chapter 7

Summary and Future Research

7.1 Objective 1

Quantify the proportion of soybean rust spores (and particles) caught inside the canopy that escape the canopy throughout the growing season and relate this value to turbulence and canopy structure.

- Spore or particle escape was greater in open canopies than in closed canopies.
- Spore or particle escape was greater in diseased fields than in healthy fields.
- Collection (or rotorod) height, mechanical turbulence, the Monin-Obukhov stability parameter, LAI, and open or closed canopy are were important predictor variables for spore or particle escape.
- The interaction between LAI and the stability parameter, LAI and mechanical turbulence, and canopy type and turbulence were important interactions.
- Spores and particles showed no difference when modeled over the entire project period.

7.2 Chapter 2

Create concentration profiles of spores and particles and estimate vertical fluxes out of the canopy

- Concentration profiles of spores and particles appeared to be logarithmic.
- Vertical escape flux of spores from a severely diseased soybean field increased with increasing mechanical turbulence.
- Vertical escape flux of particles from the same severely diseased soybean field increased with increasing mechanical turbulence, although the relationship was not as strong as for spores.
- Vertical escape fluxes of particles and spores were similar in the open canopy experiments in Florida despite 20 times more particles released per trial than spores indicating similar gradients and diffusivities between spores and particles
- Vertical escape flux of particles in the Pennsylvania experiment conducted over an entire growing season showed a stronger relationship to the strength of the source than to mechanical turbulence over the time period.

7.3 Objective 3

Provide a descriptive assessment of the directional and spatial components of movement for spores and particles in and above the canopy.

- The directional transport of spores and particles appeared to respond more to the maximum wind gust rather than the prevailing wind, especially if the gust was relatively strong or occurred early in the trial.
- If the maximum wind gust occurred late in the trial, and particularly if the gust was in a different direction than the prevailing wind direction, the tower in the direction of the prevailing wind typically had profiles of spores or particles of the same order of magnitude, if not greater, than the tower in the direction of the maximum gust.
- Crosswind and upwind transport decreased relative to downwind transport of spores or particles as prevailing winds and wind gusts increased.
- Crosswind and upwind transport relative to downwind transport increased with height.
- Ventilated canopies appeared to split the air flow above the foliage and through the lower portion of the canopy rather than pushing all incoming air currents over the canopy.

7.4 Future Research Questions

Future researchers should want to correlate these results with synoptic scale environmental variables and LAI to improve synoptic scale modeling of soybean rust (and other aerially dispersed pathogens) transport. Also, measurements were typically taken in light to moderate winds and generally pleasant, sunny weather. Measurements

in high winds and more inclimate weather may prove to be valuable in further understanding the overall transport process.

Chapter 8

List of Symbols

Symbol	Description	Units
C	concentration	spore (particles) m^{-3}
c	mass of carbon dioxide per mass of air	dimensionless
Cp	heat capacity at constant pressure	J K^{-1}
D	displacement height	m
d	rotorod head diameter	m
F_p	flux of particles	particles m^{-2} s^{-1}
F_s	flux of spores	spores m^{-2} s^{-1}
g	acceleration of gravity	m s^{-2}
H	height of the rotorod	m
H_0	surface heat flux	W m^{-2} s^{-1}
h	height of soybean canopy	cm or m
K	eddy diffusivity	m^2 s^{-1}
k	von Karmen constant	dimensionless

L	Obukhov length	m
N_0	Spore number	#
P	planetary boundary layer height	m
Symbol	**Description**	**Units**
p	spore (or particle) count	#
q	mass water vapor per unit mass moist air	dimensionless
RH	relative humidity	%
S	calculated sonic anemometer wind speed	$m\ s^{-1}$
S_x	radius of spore cloud	m
s	spore survivorship	dimensionless
T	mechanical turbulence	$m^2\ s^{-2}$
T_a	air temperature	°C
T_s	sonic anemometer virtual temperature	°C
t	time	min
Uz	vertical velocity at height z	$m\ s^{-1}$
u	downwind velocity	$m\ s^{-1}$
u*	friction velocity	$m\ s^{-1}$
V	volume	m^3
V_{sN}	settling speed for a cluster of N spores	$m\ s^{-1}$
v	crosswind velocity	$m\ s^{-1}$
v_w	wet deposition velocity	$m\ s^{-1}$
W	rotorod width	m
w	vertical velocity	$m\ s^{-1}$

wdr	wind direction	degrees
wsp	wind speed	$m\ s^{-1}$
Y	spore or particle escape proportion	dimensionless
Symbol	**Description**	**Units**
Y'	transformed escape proportion	dimensionless
z	height above surface z	m
z_0	roughness height	m
δ	spore deposition rate (downward flux)	spores $m^{-2}\ s^{-1}$
ε	escape percent	%
ζ	Monin-Obukhov stability parameter	dimensionless
θ	potential temperature	K
θv	virtual potential temperature	K
λ	rotorod length	m
ρ	density of air	$kg\ m^{-3}$
σ	rotorod revolutions	min^{-1}
τ	spore dilution factor	m^{-3}
χ	kinematic Reynolds stress	$m^2\ s^{-2}$

Bibliography

Akinsanmi, O. A., Ladipo, J. L., and Oyekan, P. O. 2001. First Report of Soybean Rust (*Phakopsora pachyrhizi*) in Nigeria. Plant Disease 85:97.

Anonymous. 2005. 2005 Soy Stats Homepage. Available at the following website: http://www.soystats.com/.

Anonymous. 2006. KPSU – Penn State University Automated Weather Observation System. Available at the following website: http://www.meteo.psu.edu/~syrett/kpsu.shtml.

Arya, S. P., 2001: *Introduction to Micrometeorology*. Academic Press, 420 pp.

Aylor, D. E. 1986. A Framework for Examining Inter-regional Aerial Transport of Fungal Spores. Agricultural and Forest Meteorology 38:263-288.

Aylor, D. E., and Ferrandino, F. J. 1985. Escape of Urediniospores of *Uromyces phaseoli* from a bean field canopy. Phytopathology 75:1232-1235.

Aylor, D. E., Ferrandino, F. J. 1989. Dispersion of Spores Released from an Elevated Line Source within a Wheat Canopy. Boundary-Layer Meteorology 46:251-273.

Aylor, D. E., and Taylor, G. S. 1983. Escape of *Peronospora tabacina* Spores from a Field of Diseased Tobacco Plants. Phytopathology 73:525-529.

Bromfield, K. R. 1984. Soybean Rust, Monograph No. 11. American Phytopathological Society. St. Paul, MN.

Caldwell, P. and M. Laing, 2001. Soybean rust - A new disease on the move. Available at the following website: http://www.saspp.co.za/.

Carmona, M. A., Gally, M. E., and Lopez, S. E. 2005. Asian Soybean Rust: Incidence, Severity, and Morphological Characterization of *Phakopsora pachyrhizi* (Uredinia and Telia) in Argentina. Plant Disease 89:109.

Davis, J. M., Main, C. E., and Nesmith, W. C. 1990. The Aerobiological Aspects of the Occurrence of Blue Mold in Kentucky in 1985. In Main, C. E. and Spurr, H. W. Jr. (eds), *Blud Mold Disease of Tobacco*. Delmar: Charlotte, NC, pp. 55-71.

DayGlo Products: NightGlo Glow-In-The-Dark Pigment. 2005. Retrieved 5 January, 2006, from DayGlo Products web site: http://www.dayglo.com/products_nightglo.asp.

Dorrance, A. E., Draper, M. A., and Hershman, D. E., eds. 2005: Using Foliar Fungicides to Manage Soybean Rust. NC-504 Land Grant Universities Cooperating. Bulletin SR-2005.

Ferrandino, F. J., and Aylor, D. E. 1984. Settling Speed of Clusters of Spores. Phytopathology 74:969-972.

Harmon, C. L., Harmon, P. F., Mueller, T. A., Marois, J. J., and Hartman G. L. 2006. First Report of *Phakopsora pachyrhizi* Telia on Kudzu in the United States. Plant Disease 90:380.

Hartman, G. L., Miles, M. R., and Frederick, R. D. 2005. Breeding for Resistance to Soybean Rust. Plant Disease 89:664-666.

Isard, S. A. and Gage, S. H., 2001: *Flow of Life in the Atmosphere: An Airscape Approach to Understanding Invasive Organisms.* Michigan State University Press, East Lansing, MI. 240 pp.

Isard, S. A., Gage, S. H., Comtois, P., and Russo, J.M. 2005. Principles of the Atmospheric Pathway for Invasive Species Applied to Soybean Rust. BioScience 55:851-861.

Isard, S. A., Russo, J. M., and Ariatti, A. In press. The Integrated Aerobiology Modeling System Applied to the Spread of Soybean Rust into the Ohio River Valley during September 2006. Aerobiologia.

Johansson, R., Livingston, M., Westra, J., and Guidry, K. 2005. *Preliminary Estimates of U.S. Economic and Environmental Effects of Treating and Adjusting to Asian Soybean Rust*. Paper presented at the Northeastern Agricultural and Resource Economics Association's Economics of Invasive Species Workshop. (http://www.arec.umd.edu/llynch/personal%20files/NAREA-2005-Johansson-Livingston-Westra-Guidry.pdf).

Kawuki, R. S., Adipala, E., and Tukamuhabwa, P. 2003. Yield Loss Associated with Soya Bean Rust (*Phakopsora pachyrhizi* Syd.) in Uganda. Journal of Phytopathology 151:7-12.

Kemerait R.C., P. Jost, D. Sconyers, D. Phillips, J. Brock, J. Clark, and J. Kichler. 2005. Summaries of Southeastern University Fungicide Efficacy Trials. Personal Communication at the APS-National Soybean Rust Symposium, 15 November 2005, Session Two:Soybean Rust Management - Fungicides. Available at: http://www.plantmanagementnetwork.org/infocenter/topic/soybeanrust/symposium/presentations/kemerait.pdf.

Kitani, K., and Inoue, Y. 1960. Studies on the Soybean Rust and its Control Measure. Agric. Hortic. 27:907-910.

Kutner, M. H., Nachtsheim, C. J., Neter, J., and Li, W., 2005: *Applied Linear Statistics Models*. 5th ed. McGraw-Hill/Irwin., 1396 pp.

Livingston, M., R. Johansson, S. Daberkow, M. Roberts, M. Ash, and V. Breneman. *Economic and Policy Implications of Wind-Borne Entry of Asian Soybean Rust into the United States*. Outlook Report No. OCS-04D-02. Economic Research Service, U.S. Department of Agriculture. Washington DC, April 2004. Available at http://www.ers.usda.gov/Publications/OCS/Apr04/OCS04D02/.

Lowry, W. P., and Lowry II, P. P., 1989: *Fundamentals of Biometeorology*. Vol. 1. Peavine Publications, 310 pp.

Lumley, J. L., 1964: *The Structure of Atmospheric Turbulence*. Interscience Publishers, 239 pp.

Melching, J. S., Dowler, W. M., Koogle, D. L., and Royer, M. H. 1989. Effects of Duration, Frequency, and Temperature of Leaf Wetness Periods on Soybean Rust. Plant Disease 73:117-122.

Miles, M. R., Frederick, R. D., and Hartman, G. L. 2003. Soybean Rust: Is the U.S. soybean crop at risk? APSnet Feature, American Phytopathological Society. Available at http://www.apsnet.org.

Miles, M. R., Frederick, R. D., and Hartman, G. L. 2005. Symptoms, Life Cycle, and Infection Process of Asian Soybean Rust (ASR). Illinois Soybean Rust Information Center. Available at http://www.soybeanrust.org.

Rosenberg, N. J., Blad, B. L., and Verma, S. B., 1983: *Microclimate: The Biological Environment*. 2nd ed. John Wiley & Sons, Inc., 495 pp.

Rossi, R. L. 2003. First Report of *Phakopsora pachyrhizi*, the Causal Organism of Soybean Rust in the Provence of Misiones, Argentina. Plant Disease 87:102.

Rotem, J. and Aylor, D. E. 1984. Development and Inoculum Potential of *Peronospora tabacina* in the Fall Season. Phytopathology 74:309-313.

Saksirirat, W., and Hoppe, H. H. 1991. Teliospore Germination of Soybean Rust Fungus (*Phakopsora pachyrhizi* Syd.). Phytopathology 132:339-342.

Schneider, R. W., Hollier, C. A., and Whitam, H. K. 2005. First Report of Soybean Rust Caused by *Phakopsora pachyrhizi* in the Continental United States. Plant Disease 89:774.

Sinclair, J. B. 1989. Threats to Soybean Production in the Tropics: Red Leaf Blotch and Leaf Rust. Plant Disease 73:604-606.

Stull, R. B., 1988: *Boundary Layer Meteorology*. Kluwer Academic Publishers, 666 pp.

Webb, E. K., "Aerial Microclimate," Meteorological Monographs, vol. 6, No. 28, July 1965, pp. 27-58.

Woodward, F. I., and Shealy, J. E., 1983: *Principles and Measurements in Environmental Biology*. Butterworths Pulishers, 263 pp.

Yang, X. B., Royer, M. H., Tschanz, A. T., and Tsia, B. Y. 1990. Analysis and Quantification of Soybean Rust Epidemics from Seventy-three Sequential Planting Experiments. Phytopathology 80:1421-1427.

Yang, X. B., Tschanz, A. T., Dowler, W. M., and Wang, T. C. 1991. Development of Yield Loss Models in Relation to Reductions of Components of Soybean Infected with *Phakopsora pachyrhizi*. Phytopathology 81:1420-1426.

Yorinori, J. T., Paiva, W. M., Frederick, R. D., Costamilan, L. M., Bertagnolli, P. F., Hartman, G. E., Godoy, C. V., and Nunes, J., Jr. 2005. Epidemics of Soybean Rust (*Phakopsora pachyrhizi*) in Brazil and Paraguay from 2001 to 2003. Plant Disease 89:675-677.

Appendix A

Monin-Obukhov Stability Theory

The Monin-Obukhov Similarity Theory (MOS) is a semi-empirical framework for a quantitative description of the mean turbulent structure of the stratified surface layer of the atmosphere. The theory states that in a horizontally homogeneous air layer, the mean flow and turbulent characteristics depend only on four independent variables: z, the height above the surface; χ/ρ, the surface drag; $H_0/\rho Cp$, surface kinematic heat flux; and $g/\theta v$, the buoyancy. The surface drag captures the frictional effects on the moving air of the surface below, the heat flux represents the addition of energy to this airflow while the buoyancy quantifies the tendency of the air parcel to move vertically due to differences in density between itself and the surrounding air. The height above the surface was taken as the measurement height of the sonic anemometer.

Some assumptions must be made in order to apply the MOS theory. The assumptions are that the flow is horizontally homogeneous and quasi-stationery, turbulent fluxes of momentum and heat are constant and independent of height, molecular exchanges are insignificant in comparison with turbulent exchanges, the rotational effects of the Earth can be ignored in the surface layer, and the influence of the surface layer roughness, boundary layer height, and geostrophic wind are accounted for in χ/ρ (Arya, 2001 and Stull, 1988).

The stability parameter ζ is estimated by

Equation **A.1**

$$\zeta = z/L \qquad \text{Eq. } \mathbf{A.1}$$

where L is the Obukhov Length. The parameter ζ is derived as the ratio of buoyant production to mechanical production of turbulence and is considered to have a stronger theoretical basis than the Richardson number (Rosenberg et al., 1983).

The Obukhov Length, L, is a characteristic height scale that represents the thickness of the air layer of dynamic influence near the surface in which shear or friction effects are always important. When $z << L$, shear typically dominates, and when $z >> L$, buoyancy dominates (Arya, 2001 and Stull, 1988).

Equation **A.2**

$$L = -u^{*3}/[k(g/\theta v)(H_0/\rho Cp)] \quad \text{Eq. } \mathbf{A.2}$$

where θv is the virtual potential temperature (K) and k is the von Karmen constant, a dimensionless number whose exact value is unknown but has been shown experimentally to range between 0.35 and 0.42. For most purposes, a value of 0.4 is assumed (Stull 1988).

The buoyancy term, g/θv, is the ratio of the acceleration due to gravity, g, and the virtual potential temperature, θv. Potential temperature is the temperature that an unsaturated parcel of dry air would have if brought adiabatically from its original state to a standard pressure, usually 1000 mb. Potential temperature is conserved for all adiabatic processes. The virtual potential temperature is defined as the theoretical potential temperature of dry air that would have the same density as moist air, making it possible to apply the ideal gas law for moist air in the same manner as for dry air. The sonic virtual temperature, T_s, is used as a substitute for θv since the sonic anemometer measurements are taken within the lowest 2.0 m of the atmosphere. Differences between T_s and θv are only on the order of 0.1°C.

The heat flux, $H_0/\rho Cp$, can be estimated as

Equation **A.3**

$$H_0/\rho Cp = w'\theta v' \quad \text{Eq. } \mathbf{A.3}$$

where w'θv' is the average covariance of the deviation from the mean vertical velocity w' and the deviation from the mean virtual potential temperature θv'.

Surface drag can be estimated by incorporating the friction velocity, u*. Friction velocity is a reference wind velocity associated with a relationship between the Reynolds stress, the mean force (per unit area) imposed on the mean wind flow by turbulent fluctuations, and the density of air. The downwind velocity component, u, and the crosswind velocity component, v, are used to calculate a scalar wind speed S where

Equation **A.4**

$$S = \sqrt{(u^2 + v^2)}. \qquad \text{Eq. } \mathbf{A.4}$$

Now, u* can be estimated by

Equation **A.5**

$$u^* = (w'S')^{(1/2)} \qquad \text{Eq. } \mathbf{A.5}$$

where w'S' is the average estimated vertical flux of horizontal wind speed, and

Equation **A.6**

$$u^{*3} = (w'S')^{(3/2)}. \qquad \text{Eq. } \mathbf{A.6}$$

Thus,

Equation **A.7**

$$L = (-w'S')^{(3/2)} / [k(g/\theta v)(w'\ \theta v')]. \qquad \text{Eq. } \mathbf{A.7}$$

The negative sign is included so that ζ has the same sign as the Richardson Number (Arya, 2001 and Stull, 1988). Since mechanical energy production increases downward in the atmosphere and the rate of buoyant production does not, at low levels (eg., < 2.0 m), the effect of buoyancy is usually small and thus values of |L| are greater than unity (Lumley, 1964).

Appendix B

Data Tables – Concentration Profiles

Table **B.1**

Tab. **B.1**: FLCs trials 1-6. Max Cov UzS is the maximum one minute average in magnitude of Cov UzS, u* is the friction velocity (m s^{-1}), B is the slope parameter from equation 4, r^2 is the fit of the data to equation 4, and Fs is the vertical flux of spores (spores m^{-2} s^{-1}).

FLCs Spore Concentrations						
Height (m)	Trial 1	Trial 2	Trial 3	Trial 4	Trial 5	Trial 6
Tower 1						
1.0	95.66	128.19	*	277.42	223.85	336.73
1.5	43.82	66.68	*	64.78	70.49	127.65
2.5	1.9	15.2	*	17.1	15.2	30.41
Max Cov UzS	-0.063	-0.035	-0.092	-0.089	-0.151	-0.193
u* (m/s)	0.251	0.187	0.303	0.298	0.389	0.439
B	-52.35	-63.05	*	-147.8	-117.8	-172.4
r^2	1.000	1.000	*	0.915	0.956	0.977
Fs	5.26	4.72	*	17.63	18.31	30.29
Tower 2						
1.0	130.42	69.93	166.33	224.92	221.14	124.75
1.5	60.89	49.47	102.75	34.25	72.31	36.15
2.5	17.16	20.97	22.88	20.97	7.63	13.35
Max Cov UzS	-0.063	-0.035	-0.092	-0.089	-0.151	-0.193
u*	0.251	0.187	0.303	0.298	0.389	0.439
B	-63.48	-27.1	-79.54	-116.6	-120.3	-63.15
r^2	0.994	0.978	0.986	0.841	0.972	0.927
Fs	6.37	2.03	9.65	13.91	18.70	11.10
Tower 3						
1.0	244.95	24.68	315.2	231.65	330.39	102.54
1.5	18.91	68.07	134.25	172.07	141.82	51.05
2.5	9.53	32.39	34.29	15.24	62.87	26.67
Max Cov UzS	-0.063	-0.035	-0.092	-0.089	-0.151	-0.193
u*	0.251	0.187	0.303	0.298	0.389	0.439
B	-134.8	*	-157.7	-118.7	-150.8	-42.69
r^2	0.792	*	0.988	0.908	0.969	0.978
Fs	13.53	*	19.13	14.16	23.44	7.50
Tower 4						
1.0	112.68	116.56	452.66	435.18	994.68	584.76
1.5	47.57	45.67	146.51	137	285.42	102.75
2.5	83.34	39.77	34.1	28.41	15.15	60.61
Max Cov UzS	-0.063	-0.035	-0.092	-0.089	-0.151	-0.193
u*	0.251	0.187	0.303	0.298	0.389	0.439
B	-18.1	-43.87	-236.3	-229.7	-552.8	-299.4
r^2	0.248	0.848	0.958	0.957	0.961	0.851
Fs	1.82	3.28	28.67	27.41	85.92	52.61

Table **B.2**

Tab. **B.2**: FLCs trials 7-12. Max Cov UzS is the maximum one minute average in magnitude of Cov UzS, u* is the friction velocity (m s^{-1}), B is the slope parameter from equation 4, r^2 is the fit of the data to equation 4, and Fs is the vertical flux of spores (spores m^{-2} s^{-1}).

FLCs Spore Concentrations						
Height (m)	Trial 7	Trial 8	Trial 9	Trial 10	Trial 11	Trial 12
Tower 1						
1.0	24.87	428.56	374.99	520.4	260.2	262.11
1.5	53.35	116.22	102.88	247.67	60.97	121.93
2.5	1.9	41.81	24.71	34.21	22.8	9.5
Max Cov UzS	-0.061	-0.129	-0.166	-0.108	-0.043	-0.087
u* (m/s)	0.247	0.359	0.407	0.329	0.207	0.295
B	-11.38	-219.4	-198.3	-271.6	-134.9	-141.1
r^2	0.157	0.920	0.937	1.000	0.902	1.000
Fs	1.24	31.52	32.32	35.70	11.19	16.65
Tower 2						
1.0	24.57	272.17	500.87	262.72	107.74	170.11
1.5	19.03	43.76	74.21	51.38	47.57	47.57
2.5	3.82	36.23	15.26	24.79	19.06	7.63
Max Cov UzS	-0.061	-0.129	-0.166	-0.108	-0.043	-0.087
u*	0.247	0.359	0.407	0.329	0.207	0.295
B	-11.38	-135.2	-276.7	-135.6	-49.9	-91.86
r^2	0.903	0.818	0.878	0.871	0.978	0.948
Fs	1.24	19.42	45.09	17.83	4.14	10.84
Tower 3						
1.0	108.23	45.58	60.76	55.07	74.05	91.14
1.5	52.94	56.73	35.93	22.69	11.35	18.91
2.5	7.62	40.01	20.96	15.24	5.72	13.34
Max Cov UzS	-0.061	-0.129	-0.166	-0.108	-0.043	-0.087
u*	0.247	0.359	0.407	0.329	0.207	0.295
B	-56.16	-2.61	-22.32	-22.6	-39.03	-44.46
r^2	1.000	0.076	0.992	0.917	0.852	0.845
Fs	5.55	0.38	3.64	2.97	3.24	5.25
Tower 4						
1.0	151.53	225.36	*	396.32	167.07	*
1.5	83.72	70.4	*	123.68	66.6	*
2.5	37.88	20.83	*	24.62	17.05	*
Max Cov UzS	-0.061	-0.129	-0.166	-0.108	-0.043	-0.087
u*	0.247	0.359	0.407	0.329	0.207	0.295
B	-63.63	-115.7	*	-209.9	-84.37	*
r^2	0.997	0.946	*	0.957	0.981	*
Fs	6.28	16.62	*	27.59	7.00	*

Table **B.3**

Tab. **B.3**: FLCp trials 1-6. Max Cov UzS is the maximum one minute average in magnitude of Cov UzS, u* is the friction velocity (m s^{-1}), B is the slope parameter from equation 4, r^2 is the fit of the data to equation 4, and Fs is the vertical flux of spores (spores m^{-2} s^{-1}).

FLCp Particle Concentrations – Main Tower						
Height (m)	Trial 1	Trial 2	Trial 3	Trial 4	Trial 5	Trial 6
Main Tower						
1.0	434.72	98.28	1441.19	2326.48	4807.76	2113.69
1.5	114.17	57.08	544.57	1024.99	485.96	858.16
2.5	38.14	40.04	142.89	425.69	87.64	240.54
Max Cov UzS	-0.063	-0.035	-0.092	-0.089	-0.151	-0.193
u*	0.251	0.187	0.303	0.298	0.389	0.439
B	-225	-32.83	-731.1	-1070	-2695	-1054
r^2	0.920	0.968	0.974	0.976	0.854	0.981
Fs	22.59	2.46	88.61	127.54	419.34	185.08

Table **B.4**

Tab. **B.4**: FLCp trials 7-12. Max Cov UzS is the maximum one minute average in magnitude of Cov UzS, u* is the friction velocity (m s^{-1}), B is the slope parameter from equation 4, r^2 is the fit of the data to equation 4, and Fs is the vertical flux of spores (spores m^{-2} s^{-1}).

FLCp Particle Concentrations – Main Tower						
Height (m)	Trial 7	Trial 8	Trial 9	Trial 10	Trial 11	Trial 12
Main Tower						
1.0	509	422.82	120.53	8188.6	813.12	585.45
1.5	353.92	341.03	108.6	773.5	222.91	161.94
2.5	223.5	188.14	102.62	214.7	136.83	91.22
Max Cov UzS	-0.061	-0.129	-0.166	-0.108	-0.043	-0.087
u*	0.247	0.359	0.407	0.329	0.207	0.295
B	-159.3	-129.3	-10.07	-4558	-385.2	-281.2
r^2	1.000	0.949	0.982	0.844	0.881	0.891
Fs	15.74	18.57	1.64	599.83	31.89	33.18

Table **B.5**

Tab. **B.5**: FLOs trials. Max Cov UzS is the maximum one minute average in magnitude of Cov UzS, u* is the friction velocity (m s^{-1}), B is the slope from equation 4, r^2 is the fit of the data to equation 4, h is the canopy height, and Fs is the vertical flux of spores (spores m^{-2} s^{-1}).

FLOs Spore Concentrations – Main Tower

Rel. Height	Trial 3	Trial 4	Trial 5	Trial 6	Trial 7	Trial 8	Trial 9
Main Tower							
1.0 h	396.32	707.89	1233.63	455.35	2468.05	1276.12	590.6
1.5 h	106.56	293.4	626.02	243.86	1880.41	884	176.96
2.5 h	98.49	214.74	337.14	186.24	1182.04	822.87	39.77
Max Cov UzS	-0.146	-0.107	-0.144	-0.041	-0.139	-0.094	-0.035
u* (m/s)	0.382	0.327	0.379	0.202	0.373	0.307	0.187
B	-170.7	-280.3	-504.5	-152.5	-713.6	-258	-311.4
r^2	0.815	0.901	0.978	0.932	0.989	0.886	0.949
Fs	26.08	36.66	76.48	12.32	106.47	31.68	23.29

Table **B.6**

Tab. **B.6**: FLOp trials 1-5. Max Cov UzS is the maximum one minute average in magnitude of Cov UzS, u* is the friction velocity (m s^{-1}), B is the slope from equation 4, r^2 is the fit of the data to equation 4, h is the canopy height, and Fs is the vertical flux of spores (spores m^{-2} s^{-1}).

FLOp Particle Concentrations – Main Tower

Rel. Height	Trial 1	Trial 2	Trial 3	Trial 4	Trial 5
Main Tower					
1.0 h	394.1	924.7	349.7	365.43	1049.07
1.5 h	141.0	443.4	201.7	163.85	639.34
2.5 h	72.2	200.8	58.72	169.13	596.62
Max Cov UzS	-0.096	-0.139	-0.146	-0.107	-0.144
u* (m/s)	0.310	0.373	0.382	0.327	0.379
B	-182.4	-407.1	-162	-112.9	-258.2
r^2	0.932	0.982	0.998	0.777	0.860
Fs	22.60	60.71	24.75	14.76	39.14

Table **B.7**

Tab. **B.7**: FLOp trials 6-9. Max Cov UzS is the maximum one minute average in magnitude of Cov UzS, u* is the friction velocity (m s^{-1}), B is the slope parameter from equation 4, r^2 is the fit of the data to equation 4, h is the canopy height, h is the canopy height, and Fs is the vertical flux of spores (spores m^{-2} s^{-1}).

FLOp Particle Concentrations – Main Tower

Rel. Height	Trial 6	Trial 7	Trial 8	Trial 9
Main Tower				
1.0 h	373.08	1471.27	529.96	376.89
1.5 h	177.18	672.53	213.38	72.31
2.5 h	55.11	490.3	209.04	41.67
Max Cov UzS	-0.041	-0.139	-0.094	-0.035
u* (m/s)	0.202	0.373	0.307	0.187
B	-178.2	-556.7	-184.1	-191.3
r^2	0.994	0.916	0.805	0.858
Fs	14.40	83.06	22.61	14.31

Table **B.8**

Tab. **B.8**: PAp trials 1-8. Max Cov UzS is the maximum one minute average in magnitude of Cov UzS, u* is the friction velocity (m s^{-1}), B is the slope parameter from equation 4, r^2 is the fit of the data to equation 4, h is the canopy height, h is the canopy height, and Fs is the vertical flux of spores (spores m^{-2} s^{-1}).

PAp Particle Concentrations – Main Tower

Rel. Height	Trial 1	Trial 2	Trial 3	Trial 4	Trial 5	Trial 6	Trial 7	Trial 8
Main Tower								
1.0 h	772.9	138.6	598.12	317.6	47.47	*	1211.43	535.46
1.5 h	322.0	28.4	366.83	180.99	41.6	*	236.36	39.71
2.5 h	129.2	32.4	59.06	60.81	11.43	*	68.59	9.53
Max Cov UzS	-0.179	-0.046	-0.143	-0.145	-0.028	-0.127	-0.212	-0.089
u* (m/s)	0.423	0.214	0.378	0.381	0.167	0.356	0.460	0.298
B	-362.7	-61.1	-298.6	-143.2	-19.63	*	-650.1	-300.8
r^2	0.970	0.769	0.982	1.000	0.829	*	0.893	0.835
Fs	61.38	5.24	45.17	21.81	1.31	*	119.73	35.89

Table **B.9**

Tab. **B.9**: PAp trials 9-16. Max Cov UzS is the maximum one minute average in magnitude of Cov UzS, u* is the friction velocity (m s^{-1}), B is the slope parameter from equation 4, r^2 is the fit of the data to equation 4, h is the canopy height, and Fs is the vertical flux of spores (spores m^{-2} s^{-1}).

PAp	Particle Concentrations – Main Tower							
Rel. Height	Trial 9	Trial 10	Trial 11	Trial 12	Trial 13	Trial 14	Trial 15	Trial 16
Main Tower								
1.0 h	*	264.02	877	1821.39	970.3	2168.1	5297.71	18588
1.5 h	*	78.11	165.54	358.17	253.4	511.9	706.82	1670.6
2.5 h	*	15.2	38.14	49.41	202	45.5	83.62	233
Max Cov UzS	-0.181	-0.238	-0.064	-0.064	-0.161	-0.193	-0.262	-0.162
u* (m/s)	0.425	0.488	0.253	0.253	0.401	0.439	0.512	0.402
B	*	-140.6	-477.1	-1006	-439.2	-1202	-2971	-10486
r^2	*	0.951	0.897	0.910	0.842	0.935	0.876	0.849
Fs	*	27.44	48.28	101.80	70.49	211.22	608.29	1688.21

Appendix C

Regression Transformation

The transformation used for spore escape proportion Y in chapter 3 is and arcsine-square root transformation

Equation **C.1**

$$Y' = 2 * \arcsin(\sqrt{Y}) \qquad \text{Eq. } \mathbf{C.1}$$

where Y is the proportion of released particles or spores that escape a soybean canopy. Whether Y is treated as a percentage or a proportion, the results are bounded between 0 and 1 or 0 and 100 respectively (note that Y must be a proportion in order to use this transformation). This type of transformation makes the proportion an unbounded, normally distributed variable making it possible to use multivariate linear regression in a statistically proper manner (Kutner et al., 2005 p. 790). It is important to note that logistic regression could have been used for this data, but the coefficients are interpreted in terms of odds and can be difficult to interpret practically. Figures C.1 and C.2 show histograms of Y and Y' respectively, and Figures C.3 and C.4 show the probability plots of Y and Y' respectively.

Figure **C.1**

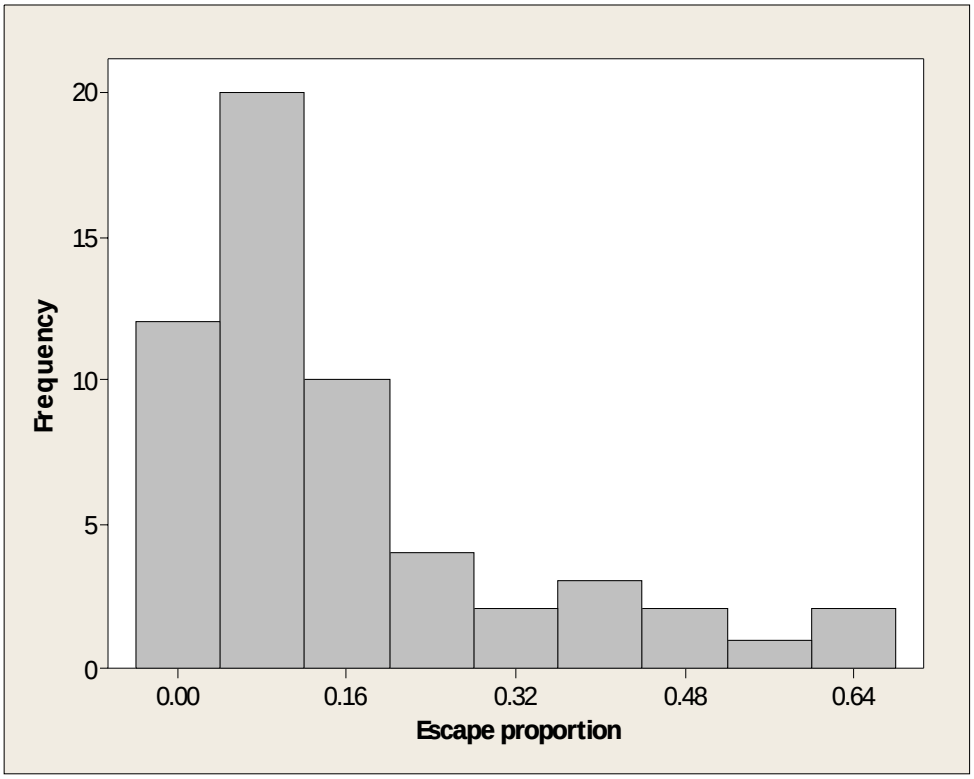

Fig. **C.1**: Histogram of escape proportion Y. The escape proportion is bound between 0 and 1.

Figure **C.2**

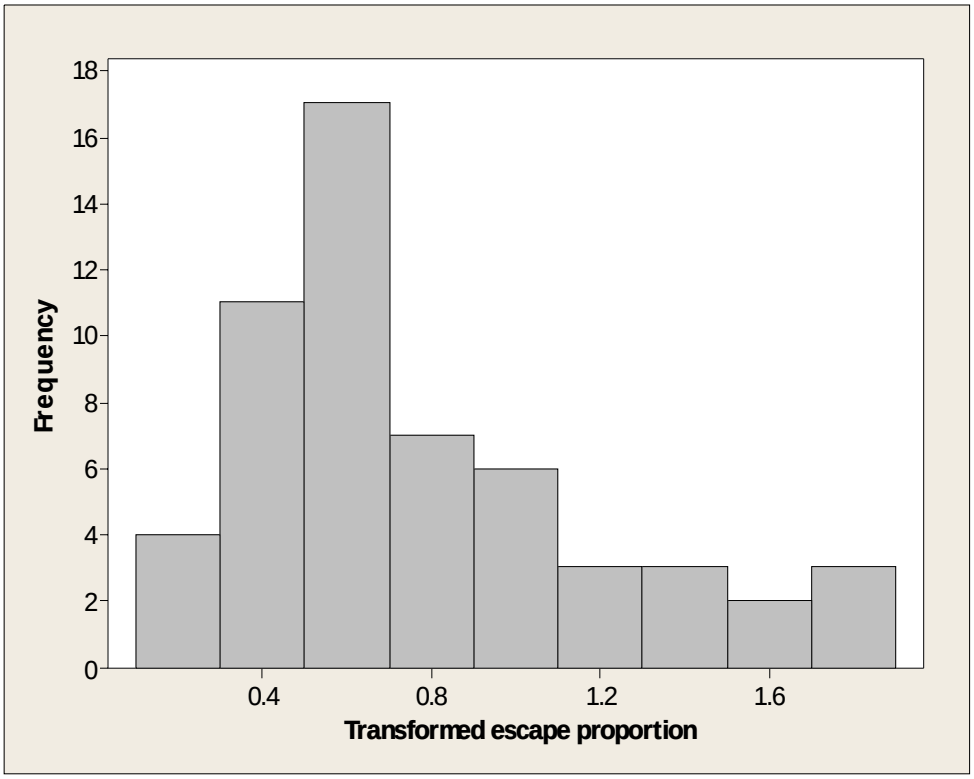

Fig. **C.2**: Histogram of transformed escape proportion Y'. The arcsine-square root transformation makes the escape proportion and unbounded, normally distributed variable.

Figure **C.3**

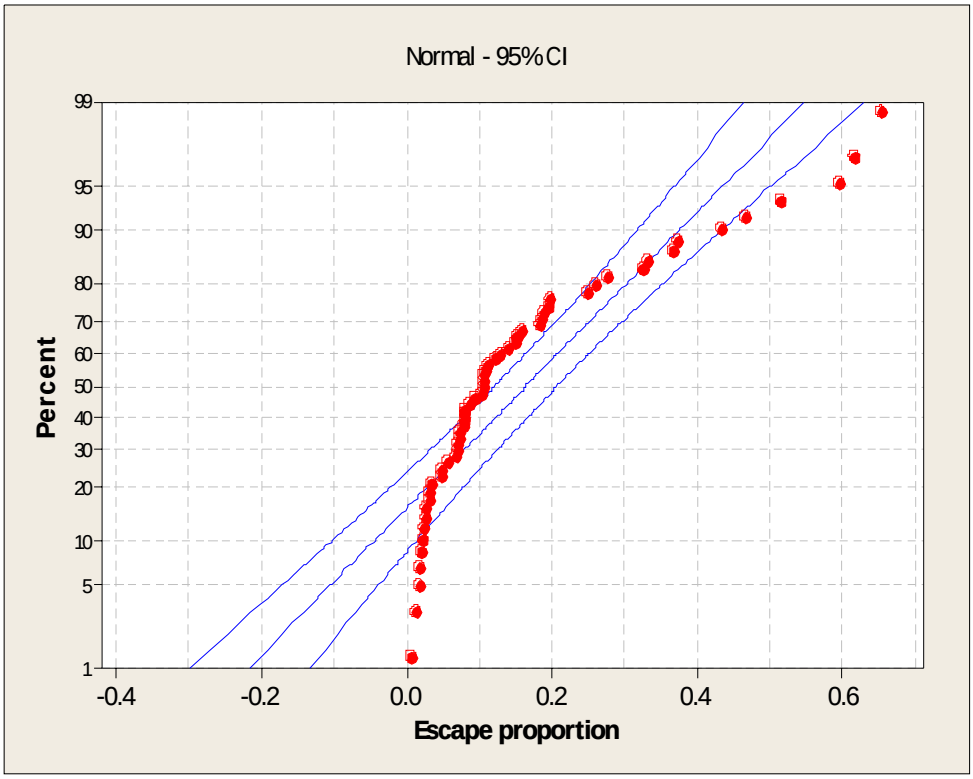

Fig. **C.3**: Normal probability plot of escape proportion Y.

Figure **C.4**

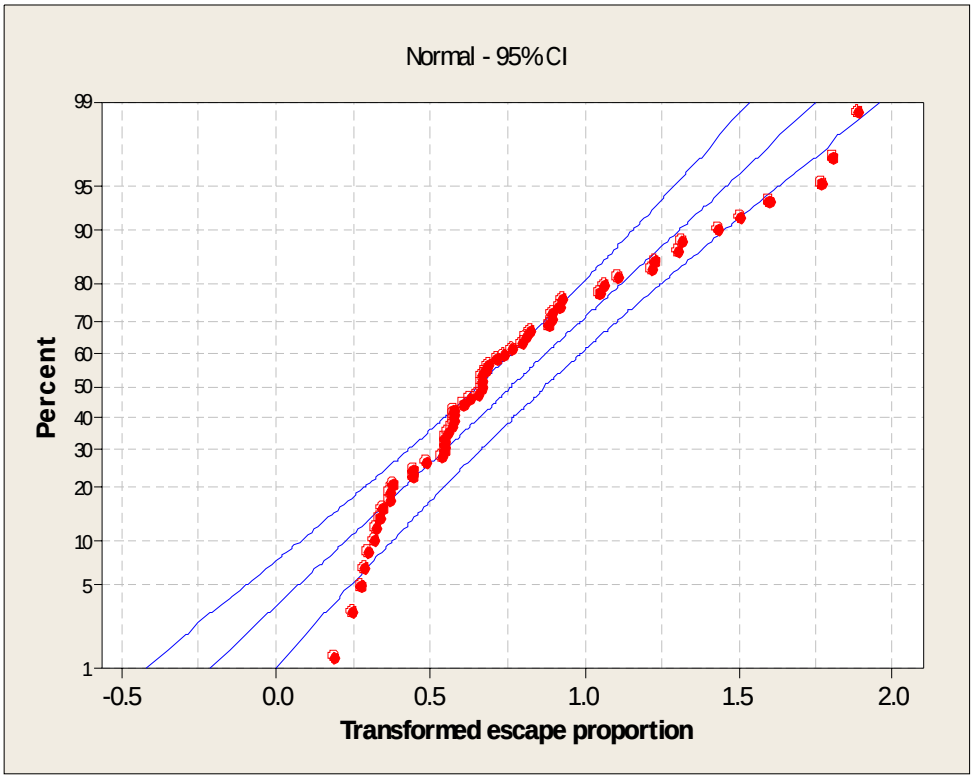

Fig. **C.4**: Normal probability plot of transformed escape proportion Y'. Note that while there are some outliers, this figure appears better than Fig. C.3.